# DECLARATION

I hereby declare all information in this document under the guidance of Dr. Ulrich Jacques DIASSO has been obtained with academic ethics and rules.

I further declare that the material and the results that are not original to this thesis are fully referenced.

# DEDICATION

To my family and to my wonderful husband KIEMDE Emmanuel.

# ACKNOWLEDGMENTS

First of all, I thank my Lord JESUS-CHRIST, for His grace and Benedictions upon my life through the master program and during my thesis work.

I would like to express my sincere gratitude to my supervisor Dr Ulrich Jacques DIASSO for his valuable guidance, his patience and his motivation. It has been a pleasured to work with him; I have learnt a lot from him.

My sincere gratitude goes to all the members of my thesis committee for their critics, comments and encouragement

My sincere gratitude to Sawadogo Windmanagda, WASCAL PhD Student in Climate Change and West Africa Climate System at the Federal University of Technology Akure (FUTA) for his contributions to this work.

I would like to thank Dr Rabani Adamou, Director of this master research program and Dr Maman Inoussa, coordinator of this master research program for their advice during the class courses and their availability.

My sincere appreciation goes to the Federal Ministry of Education and Research (BMBF) and West African Science Centre on Climate Change and Adapted Land Use (WASCAL) for providing the scholarship and financial support for this program.

I thank all lecturers for their availability and their teaching during class courses.

Finally, I express sincere thanks to my wonderful husband, to my family, to Dr Ouedraogo Joseph and his wife, and my friends for supporting me in their prayers and their encouragement to write down this thesis.

# LIST OF ABBREVIATIONS

| | |
|---|---|
| **CMIP5** | Coupled Model Intercomparison Project phase 5 |
| **$CO^2$** | Carbon dioxide |
| **CORDEX** | COordinated Regional Climate Downscaling Experiment |
| **CRU** | Climate Research Unit |
| **ECMWF** | European Centre for Medium-range Weather Forecasts |
| **ECOWAS** | Economic Community for West African States |
| **FF** | Fill Factor |
| **GCM** | Global Climate Model |
| **I** | Current |
| **INDC** | Intended Nationally Determined Contributions |
| **IPCC** | Intergovernmental Panel on Climate Change |
| **$I_{Ph}$** | Photo-current |
| **$I_{Sat}$** | saturated current |
| **$I_{sc}$** | short circuit current |
| **K** | Boltzmann constant |
| **MPP** | Maximum power point |
| **MW** | Megawatt |
| **Pmax** | maximum power |
| **PV** | Photovoltaic |
| **Pvpot** | Photovoltaic potential |
| **RCM** | Regional Climate Model |
| **RCP** | Representative Concentration Pathway |
| **RCP 4.5** | Representative Concentration Pathway 4.5 $W/m^2$ |
| **RCP 8.5** | Representative Concentration Pathway 8.5 $W/m^2$ |
| **RSDS** | surface downwelling shortwave radiation |
| **SE4ALL** | Sustainable Energy for All |
| **Si** | Silicon |
| **SRES** | Special Report on Emission Scenarios |
| **SSPs** | Shared Socioeconomic Pathways |

| | |
|---|---|
| **STC** | Standard Test Condition |
| **Ta** | air temperature |
| **$T_{cell}$** | cell Temperature |
| **TSTD** | Temperature at standard test condition |
| **TW** | Terawatt |
| **TWh** | Terawatt-hour |
| **UNFCCC** | United Nation Framework Convention on Climate Change |
| **V** | Voltage |
| **$V_{MP}$** | Voltage at maximum point |
| **$V_{OC}$** | Open circuit voltage |
| **W** | Watt |
| **Wh** | Watt-hour |
| **WMO** | World Meteorological Organization |
| **Wp** | Watt peak |
| **WSP** | wind speed |
| **µm** | Micrometer |
| **η** | Efficiency |

# ABSTRACT

The main source of electricity in West Africa comes from Fossil fuels. The fossil fuels have negative impacts on the climate system. However, this will not prevent countries to produce electricity for the welfare of their population. Renewable energy such as solar energy is the way to move forward for climate change mitigation. Nevertheless, climate change has an impact on the atmospheric variables that solar photovoltaic depend for electricity generation. In this study, we investigate the impacts of climate change on photovoltaic potential over West Africa and Ouagadougou under RCP 4.5 and RCP 8.5 in the framework of the Paris agreement. We used two Regional Climate Models (CLMcom and RCA4) from COordinated Regional Climate Downscaling Experiment (CORDEX) AFRICA initiative to analyze the impact of climate change on PV potential. These Regional Climate Models (RCMs) are driven by three Global Climate Models (CNRM, HadGEM and MPI). The PV potential was computed using surface wind speed, the air temperature and the downwelling shortwave solar radiation from the models and observation. The models were evaluated against the ERA-interim and Climate Research Unit. As result, the Regional Climate Model members and their ensemble mean are able to replicate the spatial distribution of air temperature and the surface wind speed with some biases over West Africa. In contrast, the CORDEX simulations are able to reproduce the spatial distribution of downwelling shortwave solar radiation. While, the mean surface wind speed falls in the inter quantile range of the Regional Climate Model members in the daily variation of surface wind speed over Ouagadougou, the mean air temperature and downwelling shortwave solar radiation are outside of the inter quantile range. Besides, for both global warming levels and both Representative Concentration Pathways (RCP 4.5 and RCP 8.5) all the models agree in the warming over West Africa but more effective in Representative Concentration Pathway 8.5 and in the 2 °C global warming level. Ouagadougou may experience an increase in air temperature up to 2 °C in the daily variation under both Representative Concentration Pathways and global warming levels. Different from that, there is no agreement of the models about the change in surface wind speed, downwelling shortwave solar radiation and PV potential over West Africa for both Representative Concentration Pathways and global warming levels. Finally, the inter quantile range of the Regional Climate Models project a change in the daily variation of those variables over

Ouagadougou. The results of this study will help decision-makers to plan for long term solar energy for electricity generation over West Africa and Ouagadougou.

**Keywords:** Solar energy, Climate change, Paris Agreement, CORDEX, West Africa, Burkina Faso, photovoltaic potential.

# TABLE OF CONTENTS

# LIST OF TABLES

# LIST OF FIGURES

# Chapter 1

# INTRODUCTION

## 1.1 Background

Both human-induced and natural factors influence the Earth's climate. The main factors of climate change are due to human activities (Karl et al., 2008). According to Intergovernmental Panel on Climate Change (IPCC) special report on renewable energy sources and climate change mitigation (Prof Edenhofer Ottmar, 2011); emissions from the provision of energy services contribute significantly to the increase in atmosphere greenhouse gas concentration (Prof Edenhofer Ottmar, 2011). Furthermore, the main energy sources coming from fossil fuels such as oil, coal, and natural gas contribute to global warming by greenhouse gas emissions (carbon dioxide). Nonetheless, energy sector is an important pillar in the case of sustainable development and economic growth. However, reaching the level of energy security for sustainable development and mitigate the impacts of climate change become a challenge for all countries. In other to satisfy the increase demand of energy; to preserve our environment and stabilize global warming due to human activities, 195 countries agreed to reduce the global mean temperature below 2$^{o}$C. This agreement is known as the target of the Paris Agreement in the COP 21 ( CPDN-Support Facility-Burkina, 2015). Each country renewed its commitments to the climate change convention (UNFCCC) in a document called Intended Nationally Determined Contributions (INDC) by the implementation of energy mix production or replacing conventional energy sources by renewable energy sources (solar energy, wind energy, bioenergy) for electricity generation.

Burkina Faso is one of the 195 committed countries. Burkina Faso is a landlocked country and does not have oil resources with limited rainfall. Electricity production comes from 3 sources; thermal, hydropower and imported electricity from the neighbor countries. Its electricity share is as follows: 44% from thermal power plant, 8% from hydropower and the remaining 48% from Cote d'Ivoire, Ghana and Togo in 2011. The amount of electricity produced by the electricity company was 530 GWh (147 MW) and the electricity imported from Côte d'Ivoire, Ghana and Togo was 495 GWh (138 MW) in 2011 (ME, 2016). However, the current electricity is not sufficient to meet the electricity demand in Burkina Faso. In other words, the energy demand is

greater than the energy supply. According to the government, the energy demand increases by more than 13% each year. Therefore, there is a need to produce more electricity to overcome the electricity shortage. With the Paris agreement, this production should come from renewable sources. Nevertheless, the impact of climate change on renewable energies have been widely demonstrated (Hu et al., 2016 ; Jerez et al., 2015 ; Mani & Pillai, 2010 ; Burnett et al., 2014). Although, projections are still uncertain and forecasting remains problematic. Burkina Faso's energy sector is very vulnerable to the impact of climate change. For instance, the hydropower plant electricity production may decrease in the future, which will make the country to be dependent on energy imports. In fact, 15 to 30 % shift in rainfall gradients towards the south of the country. The rainfall will be reduced by 100 mm by 2025−2050 compared to 1990-2006 baseline period (WETHE, 2009). So, we need to mix the electricity production, but produce more from renewable energy. Burkina Faso adapts energy mix strategy to increase its energy production and reduce greenhouse gas emissions by the implementation of several solar photovoltaic plants starting with Zagtouli 33 MW solar PV plants to provide Ouagadougou electricity needs. As, climate change is expected to act on the meteorological parameters which characterise the power output of photovoltaic, climate change may also impact on the PV efficiency. While PV potential can be affected by the real local weather conditions.

To know how this technology reacts under Ouagadougou real climate conditions. First, we will compare meteorological reanalysis (ambient air temperature, surface wind speed and incoming shortwave solar radiation) data to Coordinated Regional Climate Downscaling Experiment (CORDEX) data for parameter validation. Second, calculate the standard deviation to correct model bias. And at the end, calculate the future change between present days (1975-2004) and future days based on 1.5 to 2ºC global warming level under RCP4.5 and RCP8.5 scenarios.

### 1.2 Statement of problem

Most of the West Africa countries especially Burkina Faso are challenging to meet the electricity demand to satisfy their population. That challenge will continue until 2030 if there is no considerable investment in the energy sector (Vilar, 2012). In addition, the electricity access rates in the region vary from below 20% in countries like Liberia, Sierra Leone, Niger and Burkina Faso to more than 50% in Senegal and more than 70% in Ghana. Only 19% of the rural population have access to the electricity in West Africa, which is the lowest in the world (e4sv, 2016).

In other hand, most of electricity production comes from thermal power which is harmful to the environment. Despite the low emission of carbon dioxide into the atmosphere, Africa remains the most vulnerable continent to climate change which has a negative impact on the environment. However, the electricity production should come from other sources. These sources should be environmental friendly. There is a need to invest in renewable energy sources, especially in solar in West Africa. Renewable energies are free and release no harmful pollutants into the atmosphere. Therefore, the investment in renewable energy is proving a more sustainable and cost-effective path to meeting Africa's dual challenges of economic empowerment and energy access. However, climate change has an impact on renewable energy sources (Harrison and Wallace, 2005). The projection of the impact of climate change on renewable energy is very important for West Africa countries before going at large scale of renewable energy power plant. This information will help decision makers to plan the future electricity production over West Africa.

So far, there is a dearth of information on how the climate change will impact the PV potential under 1.5 and 2 °C global warming levels over West Africa and in Ouagadougou. The present study tries to address this lack of information.

### 1.3 Aim and Objective of the thesis

The aim of this work is to investigate the impacts of climate change under RCP 4.5 and RCP 8.5 scenarios in both global warming levels over West Africa, especially in Ouagadougou.

Specifically, the study aims:

1. To evaluate the CORDEX members' output with the reanalysis data over West Africa;
2. to evaluate the CORDEX members' output with the reanalysis data over Ouagadougou;
3. To show by simulation to what extent can climate change affect the photovoltaic solar energy potential in future scenarios for 1.5 and 2ºC global warming levels over West Africa.
4. To show by simulation to what extent can climate change affect the photovoltaic solar energy potential in future scenarios for 1.5 and 2ºC global warming levels over Ouagadougou.

## 1.4 Research questions

The study will address the following question:

What could be the impacts of climate change on monocrystalline photovoltaic (PV) power in future under the Paris agreement (i.e. global warming levels 1.5 and 2°C)?

## 1.5 Significance of study

Burkina Faso, a Sahelian country in West Africa, faces a high energy demand due to the development of economic activities and population growth. In 2012, Burkina State joined the UN Secretary General's SE4ALL "Sustainable Energy for All" initiative. This initiative is based on three pillars: ensuring universal access to modern energy services; to double the overall rate of improvement of energy efficiency; and give a significant share to Renewable Energies in the energy mix. Burkina Faso is also involved in the implementation of regional policies on renewable energies. As the country's has a high solar energy potential with average daily sunshine, estimated between 5.5 to 6 Kwh/$m^2$. The state begins to implement solar photovoltaic plant around Ouagadougou and in the future extend this implementation over the country. However, PV system is rated at a standard condition different from the actual environmental condition on which is set. So, one must investigate the behavior of such a system under real climate condition. This study would provide enough information on how solar photovoltaic technology will react under real climate in the future and that can help energy planners and policy makers to avoid unexpected surprises in the coming years.

## 1.6 Structure of the thesis

The thesis is composed of five (5) chapters. The introduction represents the first chapter. The second chapter, literature review associated on Photovoltaic (PV) energy, principle of PV, climate change scenario and global warming levels. The third chapter presents in details the methodology used in this study. However, the evaluation of CORDEX simulations over West Africa and Ouagadougou in Burkina Faso are exposed in the fourth chapter. In addition, the impact of climate change on PV is discussed as figures. In the last chapter of this thesis, conclusions and recommendations, a brief summary of the thesis and some recommendations are given.

# Chapter 2

# LITERATURE REVIEW

## 2.1 Different sources of Energy in West Africa (green and Non green Energy)

West African countries together form a part of the Economic Community for West African States (ECOWAS). ECOWAS comprises of 15 countries in the region with a total population in excess of 340 million. With 10,000 MW as a total electricity generation, 70% of ECOWAS population have access to electricity (Vilar, 2012). In 2011, among an estimated average of 60 % of the total population residing in rural areas only 19% has access to electricity (Vilar, 2012). Biomass (firewood and charcoal) are the main sources of energy for cooking; and hydropower, coal and oil (fossil fuels) are the main sources of energy for electricity generation in West Africa. However, renewable energy is one promising alternative to meet the ever growing electricity demand in developing countries (Tanoto et Handoyo, 2015). Diversification of energy sources are needed because is some countries, more than 90 % of electricity generation is from expensive diesel or heavy fuel. Renewable energies represent a broad and diverse array of energy resources- biomass, hydro, geothermal, wind, solar and ocean energy- as well as a range of conversion processes and applications such as combustion, thermal, mechanical, photovoltaic processes, etc. Apart from obvious emission control advantages, renewable energy technologies can also make a significant contribution to domestic energy security and spur economic development (Vilar, 2012).

## 2.2 The Photovoltaic Solar Energy: principle and technology

The most plentiful important supplier of energy for the earth is the sun. Because the sun is the starting point for the chemical and biological processes on our planet, the whole of life depends on the sun's energy. Therefore, most of energy sources (wind, fossil fuel, hydro and biomass) have their origins in sunlight. The energy released by the sun is radiated into space in the form of electromagnetic radiation; and the sun offers more energy in four hours than the human race uses in a whole year (Earthscan, 2010). Falling solar energy on the earth's surface reaches the rate of 120 petawatts, (1 petawatt = 1015 watt). Most environmentally friendly forms of all energies and

suitable for all social systems (Dinc, 2011), energy from the sun can be used in many ways by several applications for solar energy.

The direct conversion of solar energy into electrical energy is performed by means of photovoltaic (PV) generators. Generally, the term photovoltaic effect refers to the generation of a potential difference at the junction of two different materials in response to visible or other electromagnetic radiation. Photovoltaic (PV) solar technologies generate electricity by exploiting the photovoltaic effect. When light shining on a semiconductor such as silicon (Si) (the most commonly used material), electricity is generated (Sagadevan, 2013). The explanation relies on the quantum theory from Albert Einstein. Light is made up of a packet of energy called photons which energy depends on the frequency, or the wavelength of the light. For instance, the energy of the visible photons is sufficient to excite electrons bound in solids from ground energy state up to high energy states where they are free and can move.

### 2.3 Description of solar cell

A solar cell is a semiconductor p-n junction photodiode mostly made with silicon, germanium or selenium that can generate electrical power when exposed to light. There are several types of semiconductor materials used in solar cell production. The most common types known commercially are mono-crystalline, polycrystalline and amorphous silicon (Si). Like a battery, solar cell produces a continuous current, but its energy yield will be in function to the sunlight received by the cell primarily. The principal operation of a solar cell is based on the phenomenon termed as the photovoltaic effect.

The basic processes behind the photovoltaic effect are:

- Generation of the charge carriers due to the absorption of photons in the materials that form a junction,
- Subsequent separation of the photo-generated charge carriers in the junction,
- Collection of the photo-generated charge carriers at the terminals of the junction.

The photovoltaic effect was observed for the first time in 1839 by the French scientist Alexandre Edmond Becquerel. But the first real solar cell was constructed by the researchers of the Bell laboratory in the United States in 1950 (Sharma et al., 2015).

For the photons which have less energy than the energy of the band gap (which is 1.1eV for the silicon) no electrons is ejected. But when the photon has energy greater than the energy of the band gap, one electron will be moved from the valence band to the conduction band creating an electron-hole pair. The electrons created in the conduction band are able to move freely. The free electrons have to move in a particular direction by the action of the electric field present in the PV cells. These flowing electrons compose a current, which can be drawn from external use by connecting a metal plate on top and bottom of the cells. Finally, current and voltage, created because of its built-in electric field, generate electric power (Said et al., 2012). The rate of generation of electric carriers (electrons and holes) depends heavily on the flux of incident light.

### 2.4 Electrical parameters of PV solar cell

The complete behaviors of PV cells are described by five parameters (***$I_{sc}$, $V_{OC}$, $\eta$, MPP, and FF***) which is representative of the physical behavior of PV cell/module. These five parameters of PV cell/module are in fact related to two environmental conditions of solar insolation and temperature.

- **The short circuit current ($I_{sc}$)**

This is the current for which the voltage ($V$) equals zero. In the ideal case where ($R_{ser}$ =0 and $R_{sh}$ is infinite), the short circuit current is as the same as the photon current $I_{Ph}$.

$$I_{SC} = I_{Ph} - I_{Sat} * [\exp(\frac{qIR_S}{nkT}) - 1] - \frac{IR_S}{R_{Sh}} \quad [1]$$

But for most of the cases (where series resistance is too weak), we can neglect the term $I_{Sat} * [\exp(\frac{qIR_S}{nkT}) - 1]$ Vis a Vis of $I_{Ph}$. Hence, the approximate expression of the short circuit current $is$:

$$I_{SC} = \frac{I_{Ph}}{1 + \frac{R_S}{R_{Sh}}}, \quad as \quad \frac{R_S}{R_{Sh}} \lll 1 \quad [2]$$

$R_{Sh}$ is the shunt resistance, and $R_S$ is the series resistance.

Quantitatively $I_{SC}$ has the bulk value of Iph. So $I_{sc} \cong I_{Ph}$ [3]

- **Open circuit voltage ($V_{OC}$)**

The open circuit voltage is the voltage for which the current generated by the PV solar cell is equaled to zero (I=0) (the maximum voltage for a solar PV generator).

$$0=I_{Ph}-I_{Sat}*[\exp(\frac{qV_{OC}}{nkT})-1]-\frac{V_{OC}}{R_{Sh}} \quad [4]$$

In the ideal case ($R_{sh}$ infinite), its value is slightly smaller than

$$V_{OC}=nV_T ln\left(\frac{I_{Ph}}{I_{Sat}}+1\right) \quad [5]$$

- **PV solar cell efficiency**

The solar cell efficiency in terms of electricity production is the ratio between the maximum power generated by the solar cell Pmax (Iopt, Vopt) and the incident solar power.

$$\eta=\frac{Pmax}{Pinc} \quad [6]$$

Pinc is the product of the global irradiance reaching on the solar cell and the area of the cell.

$$Pinc= Ig*A \quad [7]$$

Ig is the global irradiance reaching on the cell and A is the area of the cell.

- **Maximum power point (MPP)**

The solar cell provides different capacities depending on the actual working point in which it is operated. The operating point at which the maximum power point is provided is called the maximum power point (MPP). As the power of a working point always corresponds to the surface voltage times current (V*I), this area must be maximum in the case of MPP. The current and the voltage associated with the MPP are called $I_{MPP}$ and $V_{MPP}$.

- **Fill factor FF**

The fill factor FF, describes the relationship of MPP power and the product from open circuit voltage and short circuit current. As depicted, FF shows the size of the area under the MPP working point compared to the area Voc*Isc.

$$FF=\frac{V_{MPP}*I_{MPP}}{Voc*Isc}=\frac{P_{MPP}}{Voc*Isc} \quad [8]$$

The fill factor is the measure of the quality of the cell; the closer to one (1) is the FF the higher performance the cell is. Typical values for silicon cells are between 0.75-0.85 and in the region of thin film materials they are between 0.6 -0.75.

### 2.5 Solar PV technologies

PV technologies are widely used around the world nowadays, and have various forms of application (Figure 1) such as off-grid system, hybrid systems which combine the advantage of PV and diesel hybrid in mini grids. There are three main types of PV technologies, the monocrystalline, polycrystalline and amorphous PV technologies. The series of characteristic parameters and efficiency of photovoltaic modules are given at standard test conditions (cell temperature 25°C, irradiance level 1000 W/m$^2$ at the spectral distribution of Air Mass 1.5 solar spectral content and usually obtained using solar simulators) by the manufacturers. These values cannot be used to accurately establish how much energy a module is going to produce under real sun conditions, as that depends on the specific climatic conditions of each location and on the spectral response of each technology (Cañete et al., 2014).

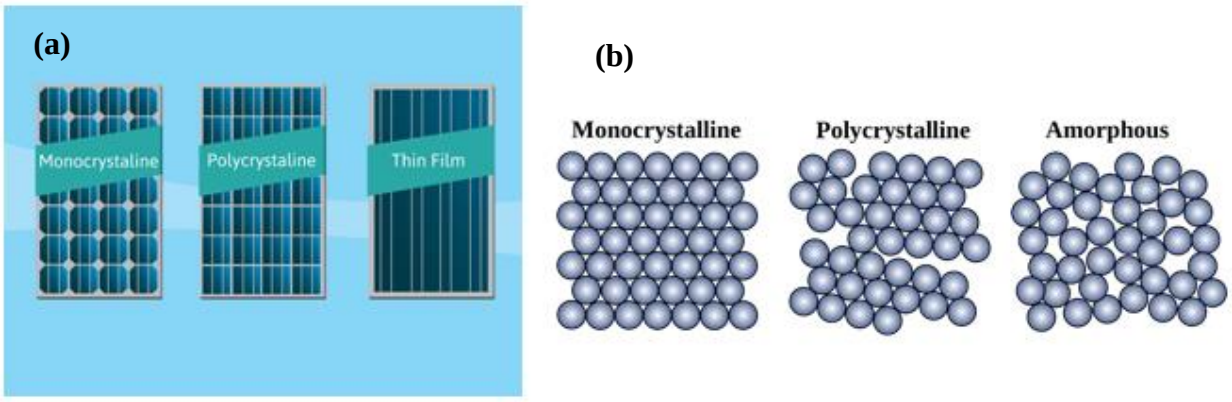

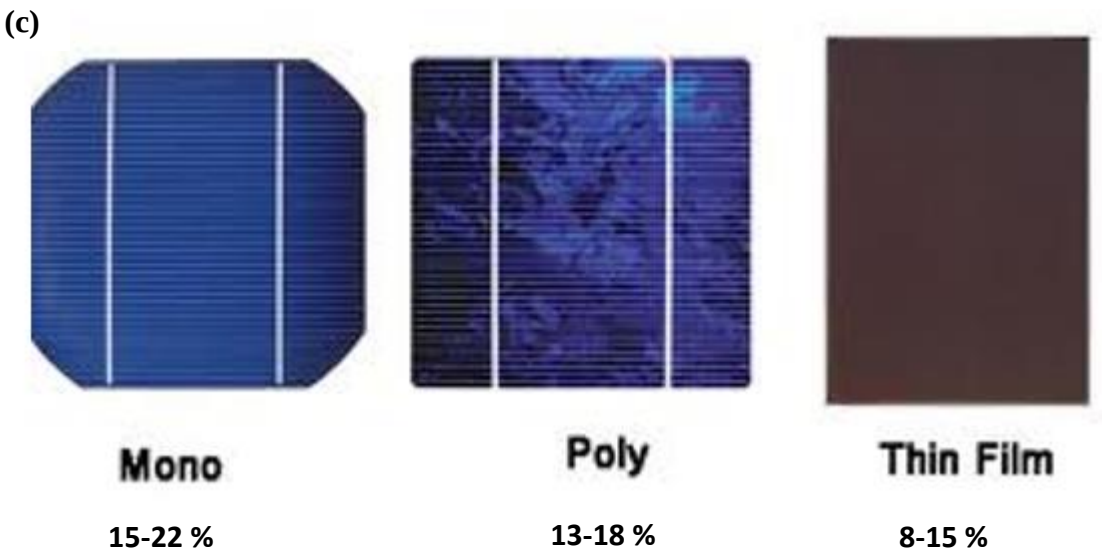


**Figure.1** *Solar PV technologies; (a) indicates solar panels; (c) represents the crystal structures and (d) is the efficiency of solar panel in industrial applications*

### 2.5.1. Crystalline technology

The crystalline technology is the most efficient PV modules available in the market. It is silicon based PV modules and comprises mono-crystalline silicon and the polycrystalline silicon. But its efficiency decreases at high operating temperature. Crystalline silicon cells are made of silicon atoms connected to one another to form a crystal lattice. This lattice comprises the solid material that forms the photovoltaic (PV) cell's semiconductors.

### 2.5.2. Mono-crystalline technology

Mono-crystalline is the oldest, most efficient PV cell technology which is made from silicon wafers after complex fabrication process (Bharam, 2012). The main properties of the mono-crystalline are cited below:

Conversion efficiency: 15 to 22%

Form: round, semi round or square,

Thickness: 0.2 to 0.3mm

Color: dark blue to black (with ARC), grey (without ARC).

### 2.5.3. Polycrystalline technology

Polycrystalline cells are made from similar silicon material except that instead of being grown into a single crystal, it is melted and poured into a mold. This forms a square block that can be cut into square wafers with less material than round single-crystal wafers. As the material cools, it crystallizes in an imperfect manner, forming random crystal boundaries. The efficiency of energy conversion is slightly lower. This merely means that the size of the finished module is slightly greater per watt than most single-crystal modules. The cells look different from single-crystal cells. The surface has a jumbled look with many variations of blue color.

The properties of polycrystalline silicon are cited below:

Efficiency: 13 to 18%,

Thickness: 0.24 to 0.3mm,

Color: blue (with ARC), silver, grey, brown, gold and green (without ARC).

### 2.5.4. Amorphous silicon

Unlike the crystalline silicon where the tetrahedral structure continues over a large range forming thus a well ordered crystal lattice, in amorphous silicon this long range order is not present. The atoms in amorphous silicon rather form a continuous random network. Moreover, not all these atoms are fourfold coordinated. In this technology, the silicon is deposited onto a backing substrate such as metal, glass or even plastic.

The main properties for the amorphous silicon PV module are:

Efficiency: 5 to 7% module efficiency (stabilized condition).

Thickness: 1mm to 3mm substrate material, with approximately 0.001mm (1μm) coating, of which approximately 0.3μm amorphous silicon.

Color: reddish brown to blue or blue-violet.

### 2.5.5. Effect of dust on PV performance

More scientists have published several papers on PV systems (Ndiaye et al., 2013; Mani & Pillai, 2010; Wild et al., 2015). With numerous studies that have been made to improve performance of such system. The studies have mainly focused on the type of PV, the effect of dust, titled angle and environmental weather conditions on the efficiency of the PV modules.

Dust is defined as particulate matter which size is less than 500 micrometers (μm) in diameter. Accumulation of dust from the outdoor environment on the panels of solar photovoltaic (PV) system is natural, especially in a Sahel where the environment is most of the time dusty. This causes high rates of dust accumulation on the solar module. Many studies have been done to assess the effect of dust on PV performance. Accumulation of dust on PV modules can reduce up to 50% the system efficiency (Sulaiman et al., 2011), dust accumulation on a glass plate tilted at 45° would reduce the transmittance by an average of 8% after an exposure period of 10 days in Roorkee, India (Garg, 1974). For (Elminir et al., 2001) dust is the major cause of depletion of direct beam solar radiation through scattering and absorption. One of the contributing factors in the drop of efficiency of solar PV panels is the accumulated dust on the panels. But the nature of the problem varies by geographical location. (Sulaiman et al., 2011) shown also under greater irradiation the effect of dust became slightly reduced but not negligible.

### 2.5.6. Effect of tilted angle

One of the methods for increasing the efficiency of the solar energy system is to use the optimum orientation and tilt angle. Some simple rules were specified for the collector tilt angle, relative only to the latitude of the location.

### 2.5.7. Effect of temperature PV cells

Most of the solar radiation absorbed by a PV module is not converted to electricity, but contributes to increase the temperature of the module thus reducing the electrical efficiency.

During the day, a solar cell operates hotter than the ambient temperature by a factor that depends on insulation. As the cell temperature increases, the short circuit current, $I_{SC}$ somewhat increases, and the maximum power, $P_{max}$ , the efficiency $\eta$ , open circuit voltage, $V_{oc}$ , and the fill factor, FF decrease (Elminir et al., 2001).

### 2.5.8. Effect of ambient temperature and irradiance, wind speed and relative humidity

Photovoltaic module manufacturers provide a series of characteristic parameters, and their efficiency. These parameters are calculated under standard test conditions (STC), the STC is defined with cell temperature 25°C, irradiance level 1000 W/m$^2$ at the spectral distribution of Air Mass 1.5 solar spectral content and usually obtained using solar simulators. These data cannot be used to accurately establish how much energy a module is going to produce under real sun conditions, as that depends on the specific climatic conditions of each location and on the spectral response of each technology (Cañete et al., 2014). Despite, the fact that irradiation is the main indicator of PV potential, it is also necessary to consider secondary parameters such as PV technology, environmental parameters (wind, temperature, humidity). They allow us to quantify with precision the amount of electricity produced by a PV system. (Elminir et al., 2001), based on experimental investigation in India, reported that ambient temperature and total irradiance intensity are the major factors that cause PV module efficiency variation. According to (Dimitri et al., 2016) solar radiation and ambient air temperature are the main inputs of PV energy production, but for more precision on PV energy estimation the effect of humidity and precipitation could be taking into account. Module temperature has significant influence on the behavior of a PV system, because it modifies system efficiency and output energy. (Harcourt, 2009), with a good working temperature of solar cells of about 43ºC, low relative humidity of about 70%, 76%, solar flux of about 78.85 kiloflux, with an open current of 18.42 x10-1A, it is possible to obtain efficiency of up to 82.28% from the solar panel. Temperature affects how electricity flows through an electrical circuit by changing the speed at which the electrons move. This is due to an increasing resistance of the circuit resulting from the rise in temperature. Therefore, resistance decreases with decreasing temperatures.

## 2.6 Climate Change and its impacts over West Africa

Climate Change from the IPCC point of view refers to any change in climate over time (usually taken over a period of more than 30 years as defined by the World Meteorological Organization,

(WMO), whether due to natural variability or as a result of human activity. The change in climate poses a big threat to West Africa's economic growth (due to changes in natural systems and resources), long-term prosperity, as well as the survival of the already vulnerable populations. The water sector is strongly influenced by, and sensitive to, changes in climate. The impacts of climate change, including changes in temperature, precipitation and sea levels are expected to have severe consequences for the availability of water in Africa. Reduction in water quantity will lead to a reduction in water quality and associated impacts on health, biodiversity, electricity generation etc. Rainfall variability is expected to increase in semi-arid and arid areas in Africa (AMCEN, 2011). Climate change, variability and associated increased disaster risks (drought, flood, heat wave, malaria) are an additional burden to sustainable development in West Africa, as well as a threat and an impediment to achieving the Millennium Development Goals.

## 2.7 Climate change Scenarios RCP4.5 and RCP8.5 and global warming levels

To limit the global mean temperature increase to below 2°C or even 1.5°C, as suggested by the Paris Agreement, abatement efforts that reach beyond industrial CO2 are also important for climate policy. More than 100 countries have adopted a global warming limit of 2°C or below (relative to pre-industrial levels) as a guiding principle for mitigation efforts to reduce climate change risks, impacts and damages (Meinshausen et al., 2009). The continued increase in the atmospheric concentration of carbon dioxide due to anthropogenic emissions is predicted to lead to significant changes in climate. Advances in climate change research, such as new scenarios known as the Shared Socioeconomic Pathways (SSPs) can provide consistent and detailed information with regard to future socioeconomic development, the abatement potentials for individual anthropogenic emissions and the corresponding costs of coping with climate change (Su et al., 2017). The need for climate change information at the regional-to-local scale is one of the central issues within the global change debate. Within CMIP5, the highest priority global model simulations have been selected to be the RCP4.5 and RCP8.5, roughly corresponding to the IPCC SRES emission scenarios B1 and A1B, respectively. Moreover, regional scenarios depend on both the global model used for driving and the choice of the regional model. The RCP4.5 and RCP8.5 scenarios are therefore also planned to be the highest priority CORDEX simulations (Giorgi et al., 2009). The first step of CORDEX project was to evaluate the capability of Regional Climate Models to reproduce the observed climate, when driven by realistic lateral conditions (Era-Interim)

and the second step was to downscale as many as possible global scenarios from IPCC-AR5 global simulations. The Representative Concentration Pathways (RCPs) form a set of greenhouse gas concentration and emissions pathways designed to support research on impacts and potential policy responses to climate change. As a set, the RCPs cover the range of forcing levels associated with emission scenarios published in the literature. Representative Concentration

Pathway (RCP) 4.5 is based on 30 satisfactory global climate models that are chosen from the Coupled Model Intercomparison Project Phase 5 correspond to a medium mitigation scenario (Sui et al, 2014) and the Representative Concentration Pathway (RCP) 8.5 corresponds to a high greenhouse gas emissions pathway compared to the scenario literature and hence also to the upper bound of the RCPs. RCP8.5 is a so-called 'baseline' scenario that does not include any specific climate mitigation target (Riahi et al., 2011). The greenhouse gas emissions and concentrations in this scenario increase considerably over time, leading to a radiative forcing of 8.5 $W/m^2$ at the end of the century.

According to (Su et al., 2017) the 2 °C target can be efficiently achieved under the assumptions of the moderate shared socioeconomic pathways 2 scenarios. However, for the 1.5 °C target, deep cuts are needed starting from the early period under the assumption of a temperature overshoot, and the efforts that are necessary to reach this target can lead to tripling the carbon price and doubling the mitigation cost compared with those in the 2 °C target case.

Solar radiation is available everywhere in our regions. So it is not cost money for its transportation and it is not pollutant. Despite solar energy seems to be infinite, the influence of environmental and meteorological conditions limits its constant provisioning. Therefore, there is a need to have a close look on how these climatic parameters influence the PV performance since the real outdoor conditions are different from the standard rated conditions of the PV modules.

### 2.8 Electricity sector in Burkina Faso

Burkina Faso is a West African country with 18 million inhabitants. Burkina Faso's electricity sector is characterized by a low access rate of 18.83% and disparities between rural areas (3.06%) and urban areas (59, 88%). The operating power of the thermal power plants connected to the interconnected national grid is 231 MW and that of the hydroelectric power plants is 26 MW as well as an import of 50 MW of the Ivory Coast. These domestic production capacities associated with imports do not cover the ever-increasing demand of around 13% per year (Jeune Afrique,

2016). This shortfall in electricity supply, especially during peak demand periods, leads to load shedding operations, thus affecting the performance of the economy and the well-being of the population. The state adapts to go through the energy mix to increase his energy production and reduce greenhouse gas emissions in order to make the country energy self-sufficient. To achieve this self-sufficient, Burkina Faso has undertaken a set of project to produce electricity from renewable sources which is illustrated in the Figure 2. However, some projects have been realized for energy production. For instance, the French president and his counterpart of Burkina Faso inaugurate in 2017 the Zagtouli solar power plant which is the biggest in West Africa and produces 33 MW. In the vision, there are some projects specifically on solar energy in many cities in Burkina Faso. Details of those projects are presented in the table 1.

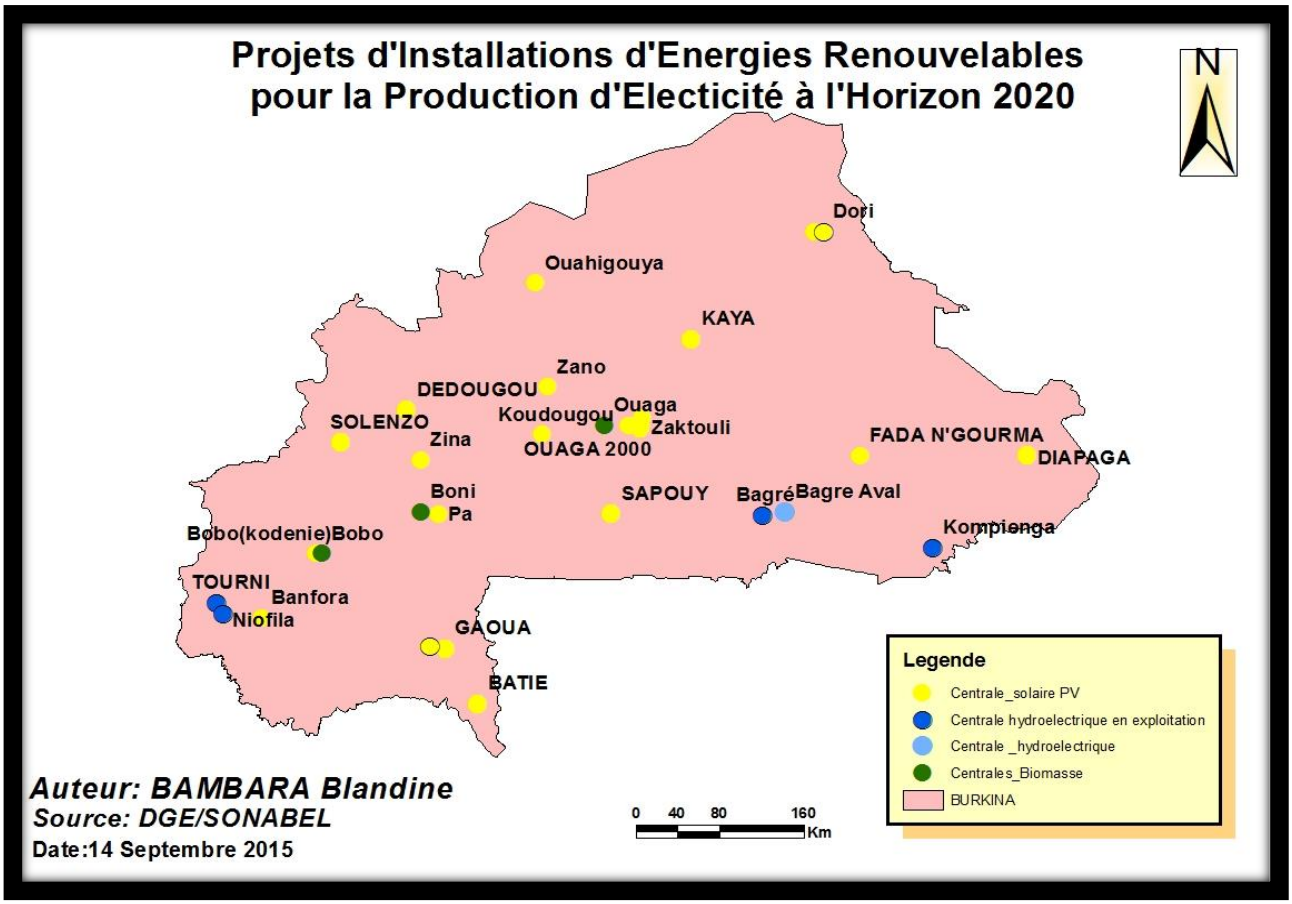


**Figure.2** *Renewable energy project for electricity production by 2020*

**Table.1** List of Burkina Faso solar photovoltaic plants project

| Location | Capacity (MWp) | Commissioning Date |
|---|---|---|
| Ziga I | 1.1 | April 2017 |
| Zagtouli I | 33.7 | September 2017 |
| Zagtouli II | 17 | 2020 |
| Koudougou | 20 | 2020 |
| Kaya | 10 | 2020 |
| Zina | 26.6 | 2020 |
| Ziga II | 17 | 2020 |
| Pâ | 17 | 2020 |
| Kodeni | 17 | 2020 |
| Patte d'Oie | 6.24 | 2020 |
| Zano | 11 | 2020 |
| Fada | 10 | 2022 |
| Dori | 15 | 2022 |
| Dedougou | 15 | 2022 |
| Ouagadougou | 30 | 2022 |
| Orodara | 10 | 2022 |
| Ouahigouya (BIDC) | 10 | 2023 |
| Site project I (AFD/BAD) | 50 | 2020 |
| Banfora | 10 | 20… |
| Site (MASEN) | 50 | 20… |

**Source: Ministry of Energy**

# Chapter 3

# METHODOLOGY

## 3.1 Study area

Our study area is the entire domain of West Africa divided into three regions (Figure 3). Those regions have been divided by Abiodun et al. (2012): Guinean zone (18W:18E, 4N:8N), Savannah zone (18W:18E, 8N:12N) and Sahel zone (18W:18E, 12N:16N). However, this study focuses specifically in Ouagadougou. Ouagadougou is the capital of Burkina Faso, administrative, cultural, communications and economic center of the nation. With 2.2 million inhabitants, Ouagadougou city's is located in the central plateau; 12.4ºN of latitude and 1.5ºW longitude. The climate of Ouagadougou (Table 2) is hot semi-arid, that closely borders with tropical wet and dry. The city is part of the Sudano-Sahelian area, with a rainfall of about 800 mm (31 in) per year. The rainy season stretches from June to September, with a mean average temperature of 28°C (82°F). The cold season runs from December to January, with a minimum average temperature of 16°C (61°F). The maximum temperature during the hot season, which runs from March to May, can reach 43°C (109°F). The harmattan (a dry wind) and the monsoon are the two main factors that determine Ouagadougou's climate. Even though Ouagadougou is farther from the equator, its hottest months' temperatures are slightly hotter than those of Bobo-Dioulasso, the second most populous city.

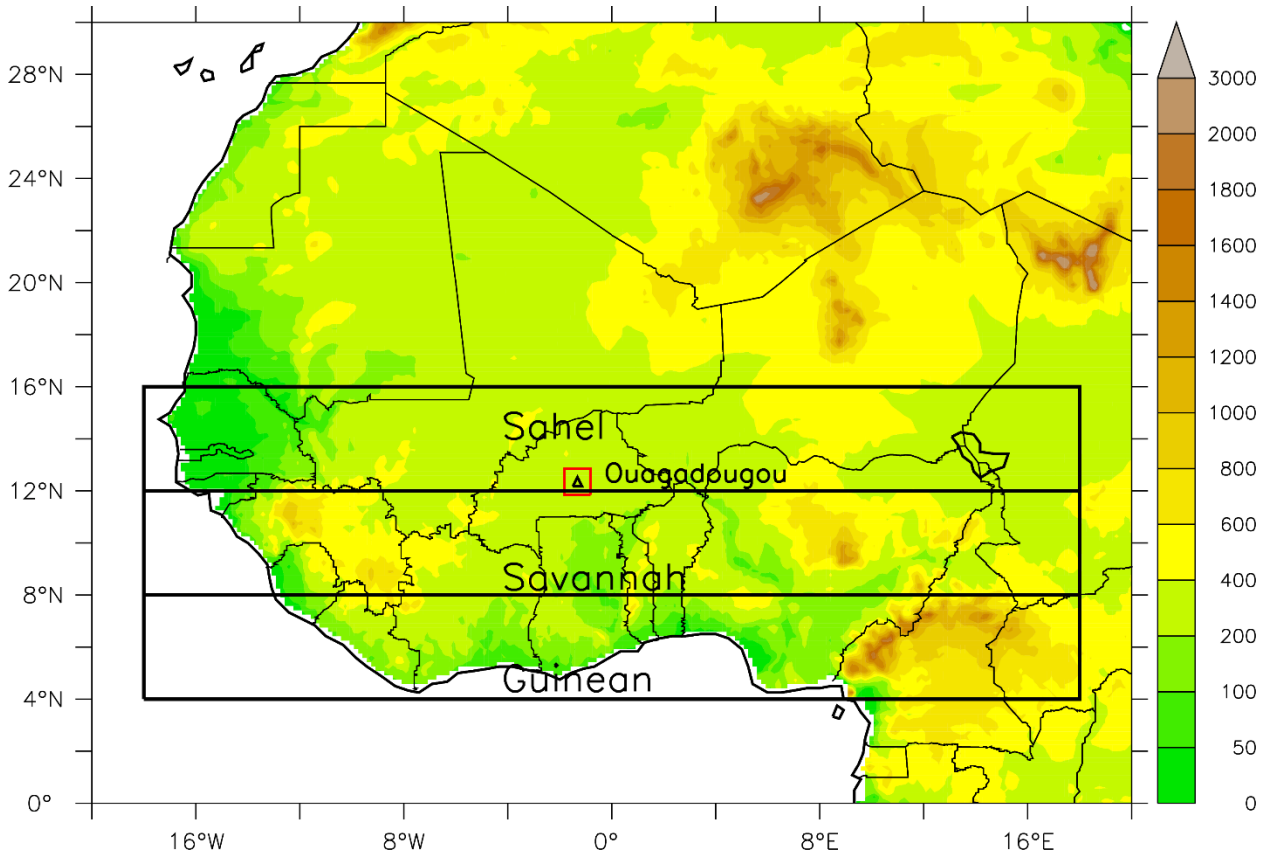


**Figure.3** *The study area showing the topography of West Africa (in meter), the three regions (black rectangle; Guinea, savanna, and Sahel) and Ouagadougou (triangle). The red boxes around it shows the area (1° x 1°).*

**Table.2** *Climate data for Ouagadougou (1971–2000, extremes 1902–present)*

| Month | Jan | Feb | Mar | Apr | May | Jun | Jul | Aug | Sep | Oct | Nov | Dec | Year |
|---|---|---|---|---|---|---|---|---|---|---|---|---|---|
| Record high °C (°F) | 39.8 (103.6) | 42.3 (108.1) | 43.8 (110.8) | 46.1 (115) | 44.5 (112.1) | 41.3 (106.3) | 38.8 (101.8) | 36.6 (97.9) | 38.6 (101.5) | 41.0 (105.8) | 40.5 (104.9) | 40.1 (104.2) | 46.1 (115) |
| Average high °C (°F) | 32.9 (91.2) | 35.8 (96.4) | 38.3 (100.9) | 39.3 (102.7) | 37.7 (99.9) | 34.7 (94.5) | 32.1 (89.8) | 31.1 (88) | 32.5 (90.5) | 35.6 (96.1) | 35.9 (96.6) | 33.4 (92.1) | 34.9 (94.8) |
| Average low °C (°F) | 16.5 (61.7) | 19.1 (66.4) | 23.5 (74.3) | 26.4 (79.5) | 26.1 (79) | 24.1 (75.4) | 22.8 (73) | 22.2 (72) | 22.4 (72.3) | 23.0 (73.4) | 19.6 (67.3) | 16.9 (62.4) | 21.9 (71.4) |
| Record low °C (°F) | 8.5 (47.3) | 10.4 (50.7) | 14.8 (58.6) | 16.2 (61.2) | 17.0 (62.6) | 17.0 (62.6) | 15.0 (59) | 17.9 (64.2) | 17.6 (63.7) | 17.6 (63.7) | 13.0 (55.4) | 9.5 (49.1) | 8.5 (47.3) |
| Average rainfall mm (inches) | 0.1 (0.004) | 0.5 (0.02) | 5.9 (0.232) | 26.5 (1.043) | 66.8 (2.63) | 97.5 (3.839) | 176.2 (6.937) | 214.2 (8.433) | 121.2 (4.772) | 33.5 (1.319) | 1.2 (0.047) | 0.2 (0.008) | 743.8 (29.283) |
| Average rainy days (≥ 0.1 mm) | 0 | 0 | 1 | 3 | 8 | 10 | 14 | 16 | 11 | 5 | 0 | 0 | 68 |
| Average relative humidity (%) | 24 | 21 | 22 | 36 | 50 | 64 | 72 | 80 | 77 | 60 | 38 | 29 | 48 |
| Mean monthly sunshine hours | 287 | 263 | 264 | 256 | 277 | 264 | 240 | 223 | 217 | 273 | 288 | 284 | 3,136 |

World Meteorological Organization,[6] Meteo Climat (record highs and lows)

### 3.2 Data

We used 3 types of dataset to conduct this study. One data is from reanalysis, the second one is from observation data and the third one is from the Regional Climate Model (RCM) simulations. ERA-Interim is the reanalysis data used in this study, which from the European Centre for Medium-range Weather Forecasts (Dee et al., 2011). The ERA-Interim reanalysis is produced with a sequential data assimilation scheme, advancing forward in time using 12-hourly analysis cycles. In each cycle, available observations are combined with prior information from a forecast model to estimate the evolving state of the global atmosphere and its underlying surface (Dee et al., 2011). The ERA Interim dataset has 0.75°x 0.75° horizontal grid size and extend from 1979 till present. From the ECMWF website, the downwelling solar radiation and the surface wind speed have been downloaded. We downloaded those variables on the daily basis. The Climatic Research Unit (CRU) is the second data used as observation in this study. We obtained the monthly air temperature, which is available from the CRU website www.cru.uea.ac.uk. The last type of data is from the CORDEX simulations (air temperature, surface wind speed and downwelling shortwave solar radiation). In fact, the CORDEX simulations has 0.44°x 0.44° horizontal grid size and his data starts from 1950 and ends in 2100. The period is subdivided in two parts. From 1950 to 2006 is the historical period and from 2006 to 2100 corresponds to the future period of the CORDEX simulations. As we considered that, the meteorological variables could act on the PV power output, the surface air temperature, the surface wind speed and the downwelling shortwave solar radiation were downloaded for each model in other to use these different variables for PVpot determination in the different equations described below. Furthermore, the CORDEX domains cover the entire African, Australian, South American, North American and European continents. The RCMs were used to downscale various global climate models (GCMs). Here, we used two RCMs and three GCMs described in the Table 3.

**Table.3** *CORDEX simulations and their 30 years period used.*

| RCM | Driving GCM | Institute | RCP 4.5 | | | | RCP 8.5 | | | |
|---|---|---|---|---|---|---|---|---|---|---|
| | | | 1.5 ˚C Global warming level | | 2 ˚C Global warming level | | 1.5 ˚C Global warming level | | 2 ˚C Global warming level | |
| | | | Start Year | End year | Start Year | End year | Start Year | End year | Start Year | End year |
| CLMcom | CNRM-CM5 | CLM | 2021 | 2050 | 2042 | 2071 | 2015 | 2044 | 2029 | 2058 |
| | HadGEM2-ES | | 2016 | 2045 | 2032 | 2061 | 2010 | 2039 | 2023 | 2052 |
| | MPI-ESM-LR | | 2006 | 2035 | 2029 | 2058 | 2004 | 2033 | 2021 | 2050 |
| RCA4 | CNRM-CM5 | SHMI | 2021 | 2050 | 2042 | 2071 | 2015 | 2044 | 2029 | 2058 |
| | HadGEM2-ES | | 2016 | 2045 | 2032 | 2061 | 2010 | 2039 | 2023 | 2052 |
| | MPI-ESM-LR | | 2006 | 2035 | 2029 | 2058 | 2004 | 2033 | 2021 | 2050 |

### 3.3 Model Evaluation

The concept of model evaluation tries to demonstrate the degree of correspondance between models and the real world where models seek to represent (Oreskes et al., 1994). Here, we evaluate a set of 6 RCM simulations carried out in the frame of CORDEX-AFRICA initiative. In other to evaluate the performance of the RCM members and their ensemble mean, observation (CRU) and reanalysis (ERA-Interim) were used to achieve that purpose. The CRU and the ERA-Interim are used to as a benchmark to assess the RCM members and their ensemble mean. Moreover, the spatial distribution, the Taylor diagram and the box plot are used to carry out the performance of the RCM members and their ensemble mean. However, for the current study, past 30 years (1971-2000) of CORDEX data were used for historical climate. The CRU and ERA-Interim data cover the same period (1971-2000). All the data have been remapped to 0.44°x 0.44°.

### 3.4 Climate change projection

The climate change projection over West Africa and Ouagadougou in this study is based on the daily basis. The RCM members are projected on the RCP 4.5 and RCP 8.5 climate change scenarios and also based in the 1.5 and 2 °C global warming level. The thirty year period of 1.5 and 2 °C global warming levels of each RCM members is obtained based in the (Déqué et al., 2017) computing. The change is obtained by doing Mean Future day minus Mean Present-day. Also we did a spatial regional assessment in other to analyze the projection change over Ouagadougou by:

- Doing an area average of the model over the city

- Analyzed the change for 1.5 and 2 °C and the spread to quantify the uncertainty by the mean of boxplot.

This is done for each variable and each model including the ensemble mean.

### 3.5 PV power potential and production

The installed capacity and the PV power generation potential (PVpot) are the two factors which depend on the PV power output at any site. As defined by (Jerez et al., 2015), the PVpot is a dimensionless magnitude accounting for the performance of the PV cells with respect to their nominal power capacity according to the actual ambient conditions. The PV power is obtained by multiplying the PVpot with the nominal installed of PV power capacity (Watt). The PVpot depends on atmospheric variables such as air temperature, wind speed and solar radiation. The PVpot is defined as:

$$PVpot = \eta_t . \frac{RSDS(W.m^{-2})}{RSDS_{STC}(W.m^{-2})}$$

Where $RSDS$ is the solar irradiance at the plane of the module/array, $RSDS_{STC}$ is the solar irradiance of 1000W/m2, $\eta_t$ is a coefficient that includes all factors that lead to the actual energy produced by a module/array with respect to the energy that would be produced if it were operating at Standard Test Condition (STC). The $\eta_t$ coefficient incorporates the distributed factors that depict the deviation of the real conditions operation of the PV array from that of the standard conditions. These factors are, the difference of the operating module (cell) temperature from the standard 25 °C. Furthermore, it also called performance ratio and it expressed as:

$$\eta_t = 1 + \gamma[T_{cell}(°C) - T_{STC}(°C)]$$

Where $T_{cell}$ is the PV cell temperature and $T_{STC}$ is the ambient air temperature at STC ie. 25 °C. $\gamma$ is the typical response of the type of the PV solar panels; in this thesis, we use a monocrystalline silicon solar panels for the simulations; $\gamma$ is taken as -0.005 °C$^{-1}$ (Jerez et al., 2015). The $T_{cell}$ modelling is based on downwelling shortwave radiation RSDS, wind speed WSP(m.s$^{-1}$) and air temperature Ta at the surface. It can be expressed as (TamizhMani et al., 2003):

$$T_{cell} = c + c_1 RSDS + c_2 T_a + c_3 WSP$$

Where c[°C], $c_1$[°C/W.m$^{-2}$], $c_2$ and $c_3$[°C/m.s$^{-1}$] are constant which depend on the type of PV module. Considering the monocrystalline silicon module the equation becomes (TamizhMani et al., 2003):

$$T_{cell} = 3.9 + 0.028 * RSDS + 0.942 * T_a - 1.509 * WSP$$

However, this methodology has been used by Jerez et al (2015) to project the impact of climate change on PV power generation in Europe.

# Chapter 4

# RESULTS AND DISCUSSION

## 4.1 Evaluation of RCM simulations over West Africa

### 4.1.1 Surface Air Temperature

Before examining the projection of the surface air temperature, surface wind speed and surface downwelling shortwave radiation, this section evaluates the capability of CORDEX RCMs by comparing their output with observed data.

The spatial distribution of the surface air temperature over West Africa is zonal (Figure 4e). In other words, the distribution of air temperature according to West Africa zones increases with latitude. Along the Guinea coast, the average surface air temperature varies from 26 to 28 $^{o}$C which represents the coldest zone over West Africa. The hottest zone over West Africa is the Sahel area where the average surface air temperature ranges from 30 to 32 $^{o}$C. Over the Savannah region, the air temperature value is between the Guinean and the Sahel zone (from 28 to 30 °C). However, all the RCMs and their ensemble mean are able to replicate the spatial distribution of surface air temperature. The correlation value varies from one RCMs to another RCMs, but all are giving a good correlation. Nonetheless, the correlation of the same driving GCMs differs with the RCMs (RCA and CLMcom). For instance, the correlation of RCA-MPI is about 0.89 whereas the correlation of CLMcom-MPI is 0.88. While the correlation of CLMcom-CNRM is 0.74, the RCA driving by CNRM is about 0.82. The RCA-HadGEM gives 0.87 as correlation value and 0.88 is the correlation value of the CLMcom-HadGEM. The ensemble mean of both RCMs has the same correlation value (r=0.86). Among the RMCs, the RCA-MPI has the highest correlation value while the CLMcom-CNRM has the lowest value. The difference between the same driving GCMs with different RCMs in terms of spatial distribution may be due to the internal configuration of the RCMs.

There is a bias between the RCMs and the CRU data. In general, there is a bias between models output and observation in the present day (Kerkhoff et al., 2014). The difference of spatial distribution between the CRU data the RCMs exhibits negative and positive bias over West Africa. The RCMs does not capture the magnitude of the air temperature over West Africa. For example,

both driving GCMs (CNRM) underestimates the magnitude of air temperature, especially in the Sahel zone indeed to 4 °C. A similar bias is observed in both ensemble mean.

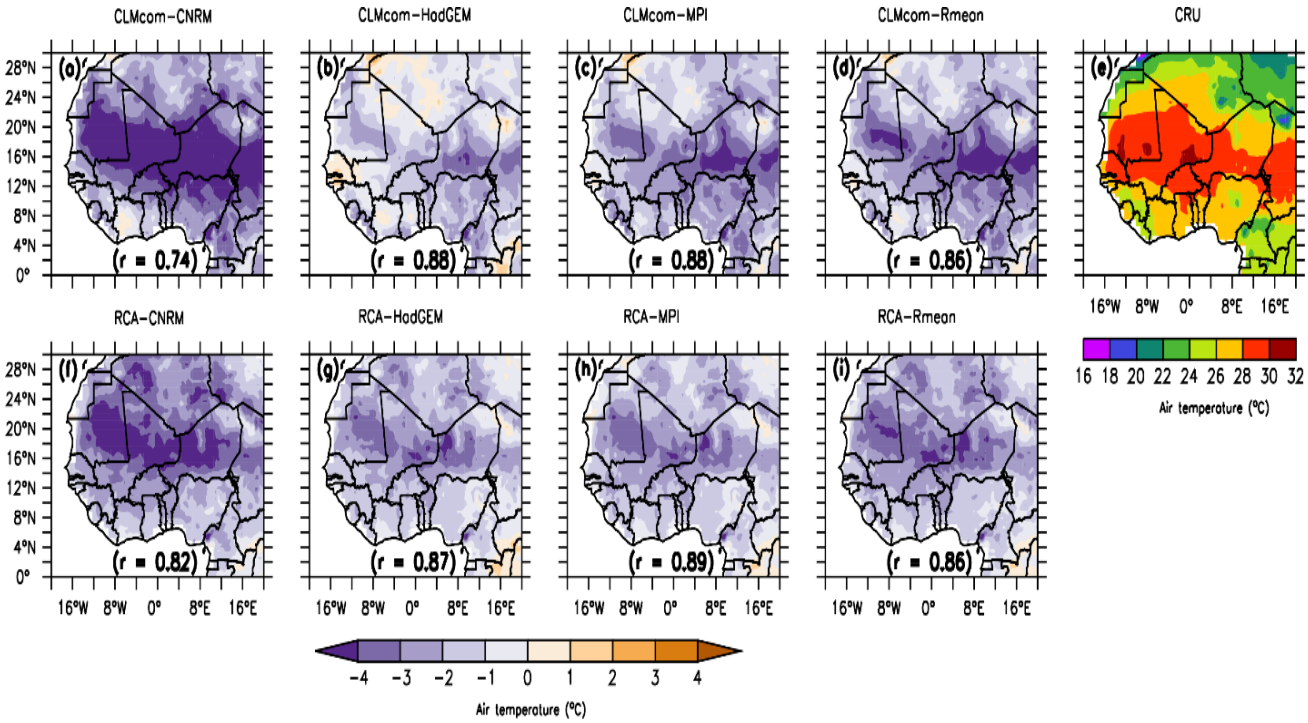


**Figure.4** *Spatial distribution of the historical period (1975-2004) of mean surface air temperature over West Africa. From (a) to (c) shows the bias of CLMcom members and (d), the ensemble mean. (f)-(h) indicate the bias of RCA members and (i) the ensemble mean. The observed data is showing in the (e).*

### 4.1.2 Surface Wind Speed

The spatial distribution of surface wind speed over West Africa is shown in Figure.5, for reanalysis data (Figure 5e), the ensemble mean for RCA (Figure 5i), the ensemble mean for CLMcom (Figure 5d), and each of ensemble RCM member (Figure 5a, 5b, 5c, 5f, 5g, 5h). The RCMs and their ensemble mean generally overestimate the surface wind speed over the Guinean and Savannah areas and underestimate it over the Sahel zone. The bias of the RCA ensemble mean is higher than the CLMcom mean over the Sahel region. In general, each RCM members show almost the same bias over the same location. However, each RCM is able to capture the spatial distribution of surface wind over West Africa. There is a good spatial correlation between the RCMs and the reanalysis on surface wind speed over West Africa. For example, the correlation of RCA-MPI is 0.88 whereas the correlation of CLMcom-MPI is 0.84. The RCA-HadGEM correlation is 0.82 and

the CLMcom driving by HadGEM is about 0.81. The RCA-CNRM gives 0.86 as correlation value and 0.84 is the CLMcom-CNRM correlation value. The ensemble mean of both RCMs has different correlation value. The correlation value of the RCA ensemble mean is about 0.86 and 0.83 for the CLMcom ensemble mean. Among the RCMs, the CLMcom-HadGEM has the lowest correlation value while the RCA-MPI has the highest value.

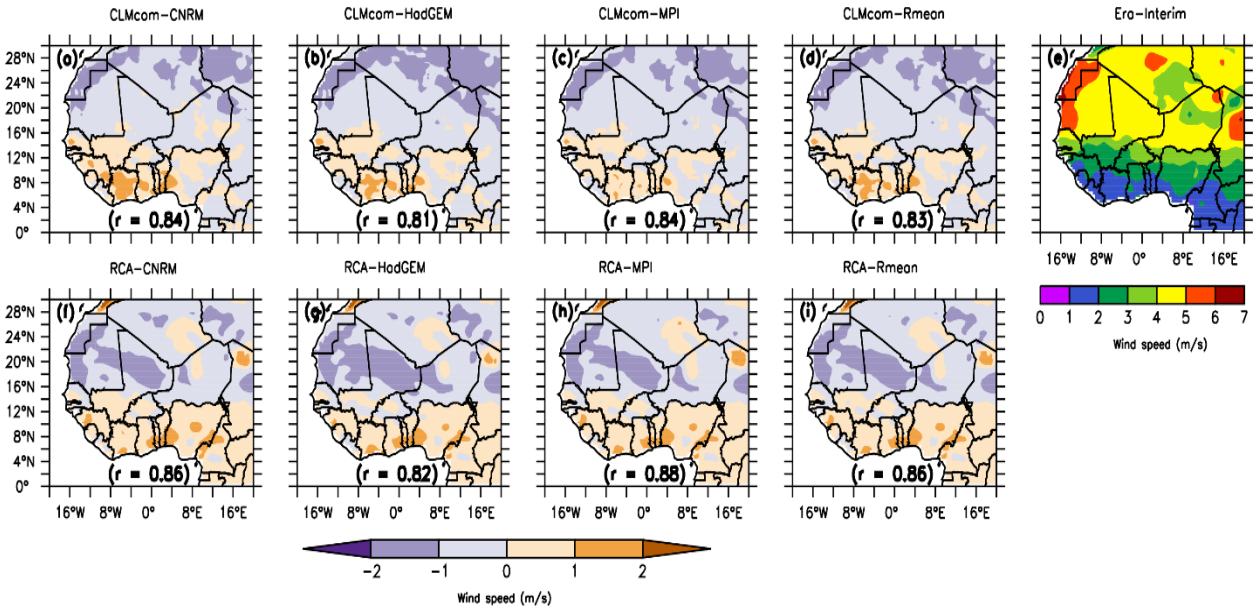


**Figure.5** *Spatial distribution of the historical period (1975-2004) of mean surface wind speed over West Africa. From (a) to (c) shows the bias of CLMcom members and (d), the ensemble mean. (f)-(h) indicate the bias of RCA members and (i) the ensemble mean. (e) indicates the ERA-Interim data.*

### 4.1.3 Surface Downwelling Shortwave radiation

The spatial distribution of surface downwelling shortwave solar radiation (RSDS) over West Africa is complexed. It increases with latitude and decreases with longitude at the same time. The variation of RSDS over the Guinea zone ranges from 60 to 120 W/m$^2$. The Guinea zone is the area which receives less RSDS. The area which receives important RSDS is Sahel region, which range from 80 to 160 W/m$^2$. Over the Savannah region, the RSDS value varies between 80 to 140 W/m$^2$. However, the RCA members (CNRM, HadGEM and MPI) is unable to replicate the spatial distribution of RSDS. The correlation between them and Era-Interim data is very poor. For instance, the correlation of RCA-HadGEM is 0.0079, RCA-MPI gives 0.044 as correlation value and the correlation value of RCA-CNRM is about -0.038. The RCA ensemble mean correlation

value is about 0.0077. Nonetheless, the CLMcom members generally are able to replicate the spatial distribution of RSDS over West Africa. The correlation value of the RCMs is as follow: CLMcom-CNRM equal to 0.6, CLMcom-HadGEM equal to 0.44 and CLMcom-MPI equal to 0.47. The mean of ensemble gives as correlation value of 0.5. Nonetheless, all the RCM members and their ensemble mean exhibit a positive bias over West Africa. In other words, all the RCM members together with their ensemble mean overestimates the magnitude of RSDS up to 200 $W/m^2$ over West Africa.

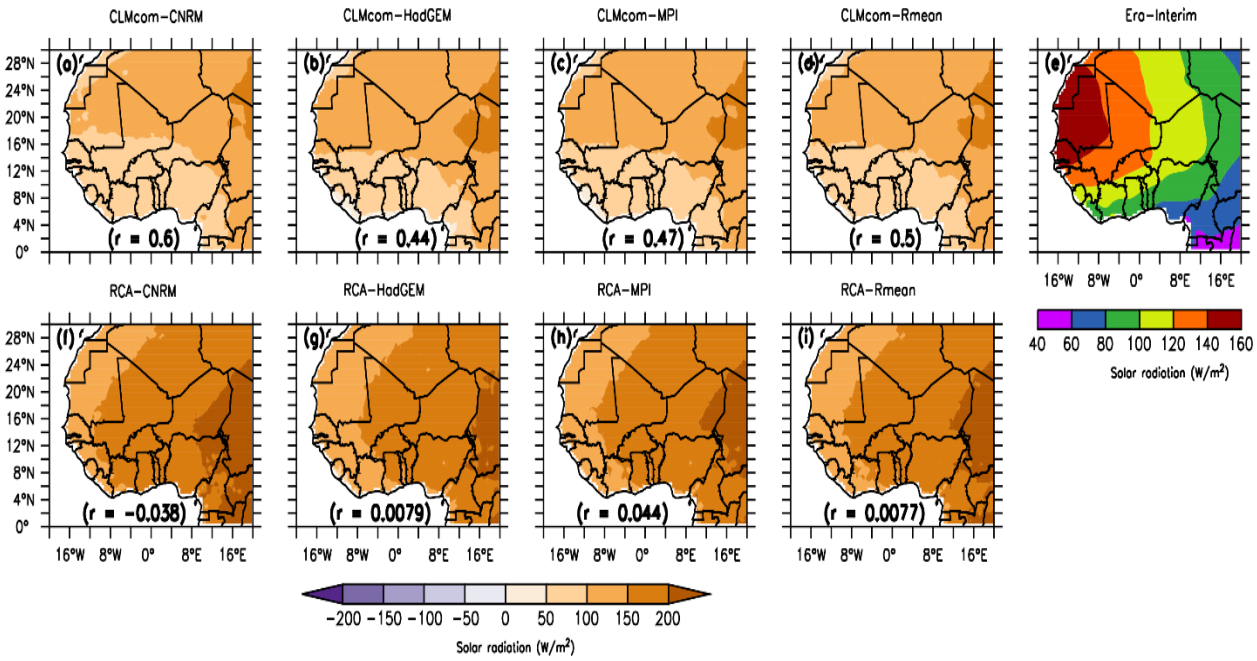


**Figure.6** *Spatial distribution of the historical period (1975-2004) of mean surface downwelling shortwave radiation over West Africa. From (a) to (c) shows the bias of CLMcom members and (d), the ensemble mean. (f)-(h) indicate the bias of RCA members and (i) the ensemble mean. (e) indicates the ERA-Interim data.*

## 4.2 Evaluation of RCM simulations over Ouagadougou

### 4.2.1 Boxplots

Conveying the normal variability of weather conditions or specific weather events can be of critical importance as a decision and planning tool for engineers, agriculturists, recreational enthusiasts, and others with weather sensitive interests. Thirty years of climate means and extremes may not be effective to demonstrate natural fluctuations in weather about the mean that are typical on daily,

seasonal, or annual time scales. Common measures of variability, such as standard deviation, are based upon the assumption of a standard normal distribution, and might also prove too abstract for non-technical users of climate data. What is often needed is a simple graphical summary that portrays the statistical dispersion in a manner that is easy to interpret for a wide range of users. Climate statistics help place observed or anticipated weather events in a historical context. One way of graphically focusing on statistical variability is by way of the box and whisker plot.

Spatial distributions of (a) surface wind speed, (b) surface downwelling shortwave radiation and (c) surface air temperature (daily mean) in Ouagadougou describe by reanalysis (Era-Interim or CRU) and RCMs simulations (1975-2004). The lines in a boxplot (from bottom) show the minimum, 25th, median, 75th and maximum values in the RCMs while the red dot shows ERA-Interim or CRU values. The model ensemble simulates strongest wind speed up to 12 m/s and weak wind speed about 1m/s (Figure 7a). In general, the RCMs produce high wind speed compared to the reanalysis. Nonetheless, the average wind speed of reanalysis at Ouagadougou falls into 50% of the RCM. The Figure 7b exhibits the spread of the RSDS. The model ensemble simulates high RSDS (up to 370 W/m$^2$). All RCM produces high RSDS than reanalysis. In other words, the RCM simulations and the ensemble mean overestimate the RSDS. In contrast, all the RCM members underestimate the air temperature (Figure 7c). The model ensemble simulates wide spread of air temperature; the values vary between 12 to 40ºC. CLMcom model results are very spread compare to RCA model results.

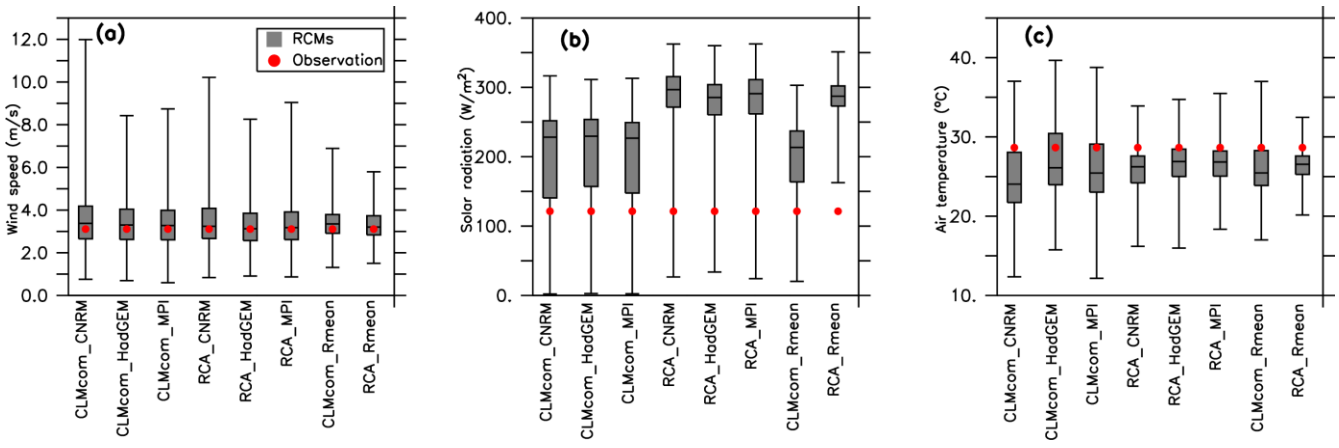


**Figure.7** *Boxplot comparing CORDEX simulation with the observed and reanalysis data. The red dot indicated the mean of the observed or reanalysis data.*

### 4.2.2 Taylor Diagrams

The Taylor diagram is a very useful diagram in climate models evaluation. And it has been widely used in model inter-comparison and evaluation studies over the several years. A common application of Taylor diagram is to compare multi-model simulations against observations in terms of the patterns of scalar fields (Davy and Esau, 2014). Taylor diagram is used to quantify the degree of correspondence between the modeled and observed behavior in terms of three statistics: the Pearson correlation coefficient, the root mean square error and the standard deviation. In this analysis, we will emphasize on the normalized standard deviation and the Pearson correlation coefficient to compare how best RCM represents observation or the reanalysis data.

The Taylor diagrams shown in this Figure 8 provide a summary of the relative skill with which several regional climate models simulate the spatial pattern and the amplitude pattern over Ouagadougou of daily surface wind speed, RSDS and surface monthly air temperature for the reference period (1975-2004). Three GCMs (CNRM, HadGEM and MPI) driving by two RCMs (CLMcom and RCA) and their ensemble mean, each of the RCM members and their ensemble mean are represented by a different dot color in the diagram. They are compared to observe and reanalysis where observe and reanalysis are in black dot. For each RCM, two statistics are plotted: the Pearson correlation coefficient (gauging similarity in pattern between the simulated and observed fields) is related to the azimuthal angle and the standard deviation of the simulated pattern is proportional to the radial distance from the origin.

It is evident from the first diagram (surface wind), that for the same driving GCMs with different RCMs and the ensemble mean of the RCMs, the correlation coefficient value is not significant. The correlation value ranges from 0 to 0.15. RCA-MPI, RCA-CNRM, CLMcom-CNRM and CLMcom-HadGEM have the same correlation coefficient and different standard deviation. Their correlation coefficient is about 0.08. CLMcom-MPI has about 0.15 as correlation coefficient which is the greater correlation coefficient among all. RCA-MPI has 1 as normalized standard deviation, CLMcom-HadGEM and RCA-CNRM normalized standard deviation is about 1.1, and 1.2 is the normalized standard deviation of CLMcom-CNRM. CLMcom-MPI has same normalized standard deviation value as CLMcom-HadGEM and RCA-CNRM. The normalized standard deviation of these RCMs is a slightly greater than the normalized standard deviation of the observed surface

wind speed. Although the ensemble mean of both RCMs have the same normalized standard deviation value of 0.7 and different correlation coefficient value.

The relative merits of various RCMs and their ensemble mean can be inferred from the first diagram. Simulated patterns that agree well with observation will lie nearest the black dot "observed" on the x-axis. These models must have relatively high standard deviation and high correlation. But in our case, any model has relatively high standard deviation and high correlation. From the diagram, it can be seen that RCA-MPI, RCA-CNRM and CLMcom-HadGEM generally agree best with observations based on the normalized standard deviation value only. RCA-MPI is the one among models, which has the normalized standard deviation value very close to one of the reanalysis. In terms of normalized standard deviation, RCA-MPI simulates better the amplitude of surface wind variation. However, CLMcom-MPI has a slightly higher correlation than others. It simulates better the spatial variation. Both RCMs ensemble mean have a low pattern correlation and low standard deviation. Note also that CLMcom-mean simulates the spatial variations (i.e., the correlation) much better than RCA-mean.

From the second diagram, the spatial variation of RSDS over Ouagadougou is underestimated with a value of less than 0.5 and the amplitude of RSDS is up to five times overestimates. Nonetheless, the normalized standard deviation of the RCA members is less than the normalized standard deviation of the CLMcom members. For instance, the normalized standard deviation of RCA-CNRM and RCA-HadGEM is 2. RCA-MPI standard deviation is about 2.2 and 1.4 is the normalized standard deviation of the RCA mean ensemble. The normalized standard deviation of CLMcom-MPI and CLMcom-CNRM are successively 4.5 and 5. The CLMcom ensemble mean normalized standard deviation is about 3.3. However, the correlation coefficient value varies from one RCM to another. The correlation coefficient value 0.4 is the correlation coefficient of RCA-CNRM and RCA ensemble mean. The CLMcom-CNRM gives about 0.35 as correlation coefficient value and the correlation coefficient value of CLMcom-MPI is about 0.3. Thus, RCA-CNRM simulates much better Ouagadougou downwelling short wave radiation because its normalized standard deviation (about 2) is closer to the observed standard deviation than CLMcom-CNRM standard deviation (about 5).

The third diagram shows two statistics (Pearson correlation coefficient and standard deviation) of the models compared to reanalysis Ouagadougou surface air temperature. The correlation

coefficient RCA members and his ensemble mean is approximatively equal to 0.8 and the normalized standard deviation is about equal to 0.8 also. Within an overall correlation coefficient value of 0.9, GCMs driving by CLMcom has approximatively about 1.6 as normalized standard deviation. In spite of the correlation coefficient of GCMs driving CLMcom is very close to 1 (ie. the correlation coefficient value of the reanalysis surface air temperature), the standard deviation of these GCMs driving CLMcom (1.6 as value) is so far to reanalysis standard deviation of Ouagadougou surface air temperature (observed surface air temperature standard deviation is 1). We can say that GCMs driving by CLMcom are good spatial variations of Ouagadougou surface air temperature and bad simulation of the amplitude of surface air temperature (overestimation of the Ouagadougou surface air temperature).

GCMs driving by RCA agree much better with the observed Ouagadougou surface air temperature because their standard deviation and correlation coefficient values are around 0.8 which the value is close to 1 in the two statistics cases. There is an agreement between GCMs driving by RCA and CRU reanalysis surface air temperature. That agreement is the capability of GCMs driving by RCA to reproduce realistic Ouagadougou surface air temperature.

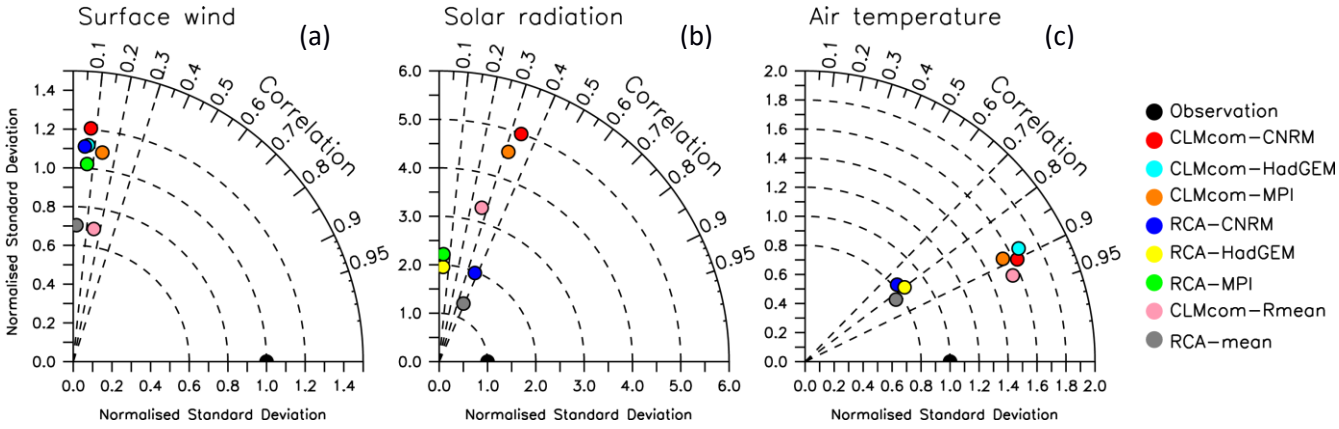


**Figure.8** *Taylor diagram illustrating correlation and normalized standard deviation for daily RCM members simulations compared to: daily wind speed (a); daily RSDS (b) and month surface air temperature (c).*

## 4.3 Climate Change Projection under RCP4.5

### 4.3.1 Change in surface air temperature

The future change of surface air temperature over West Africa for RCP 4.5 climate change scenario and 1.5 °C global warming is shown in Fig 9(a)-9(h) and 2 ºC global warming in Fig 9(i)-9(p) from the RCMs members and their ensemble mean. All the RCM members and their ensemble mean agreeing to an overall warming over West Africa for both global warming. However, the magnitude of the warming in 2 ºC is more enhanced than the 1.5 ºC. For instance, the CLMcom and the RCA RCMs driving by the same CNRM could reach the value up to 1.5 ºC for 1.5 global warming level while they could reach 2 ºC for 2 global warming level. Similar projection is found in the driving MPI for 1.5 global warming and that projection could reach the value of 2.5 ºC for the 2 ºC global warming. The driving HadGEM projects a change of 2 ºC for 1.5 global warming level and 3 ºC for the 2 global warming. The increase in temperature is more pronounce in HadGEM for both RCMs (CLMcom and RCA) and could reach 2 ºC. The warming of the spatial distribution is different for each ensemble member. Along the coast, all the RCMs exhibit a weak warming compared to the other regions. The warming core over West Africa from the RCM ensembles and their ensemble mean is generally located in the Sahel region. These results corroborate with a study undertaken by Diallo et al (2012) where the core of the future warming will be in the Sahel region and a weak warming in the Guinean area (Diallo et al., 2012). For each global warming level, the ensemble mean have a similar spatial distribution but more pronounce in the 2 ºC global warming level.

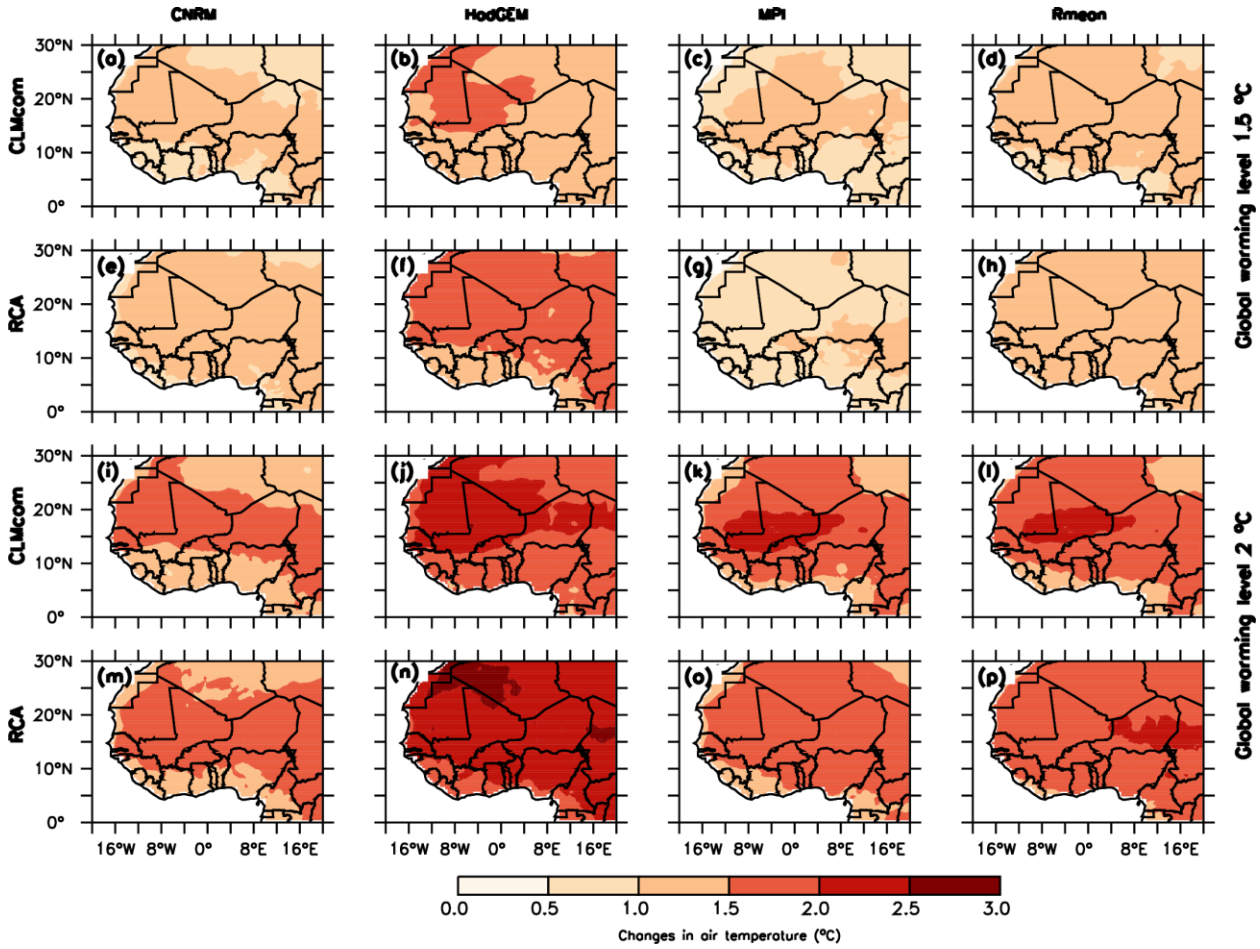


**Figure.9** *Spatial distribution of RCM members and their ensemble mean of the change in surface air temperature over West Africa of 1.5 and 2 global warming level under RCP 4.5.*

All the RCMs members and their ensemble mean project an increase of daily surface mean temperature in Ouagadougou for both global warming level (Figure 10). The projected of daily surface mean temperature generally is higher in 2 ºC global warming level than the 1.5 ºC global warming level. The CLMcom members exhibit higher minimum and maximum value than the RCA members. Most of 50% of the daily surface mean temperature of the RCM members agree to an increase of temperature in Ouagadougou for both global warming level. The threshold of that increase of daily mean temperature is less than 2 ºC for all the RCM members for 1.5 ºC global warming level. However, the CLMcom members project a maximum value above 12 ºC whereas, the RCA members project an increase less than 12 ºC for both global warming level. For both global warming levels, the ensemble mean agrees to an increase of daily surface mean temperature. Nevertheless, the CLMcom ensemble mean exhibits more increase in the daily surface mean

temperature in the 2 ºC global warming level than the RCA ensemble mean while it is the opposite in the 1.5 ºC global warming level. Nonetheless, some RCM members show 25% of the daily data a decrease of daily surface temperature over the city in both global warming level.

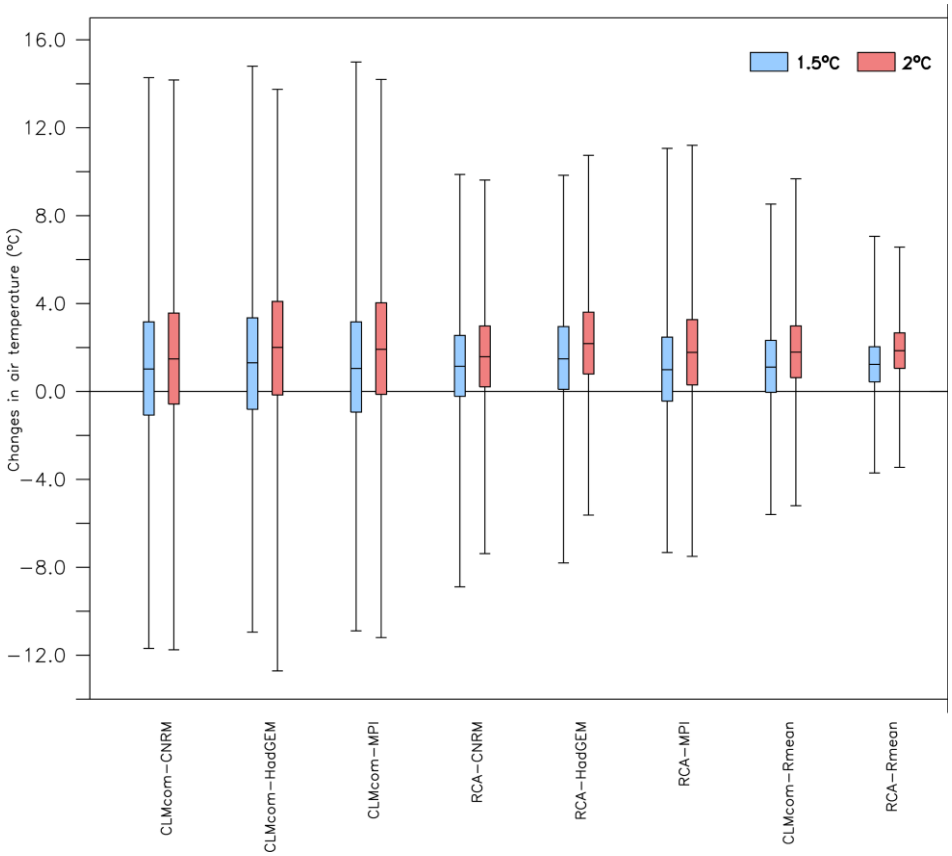


**Figure.10** *Boxplot of the change in surface air temperature of RCM members and their ensemble mean for 1.5 and 2 ºC global warming level over Ouagadougou under RCP 4.5.*

### 4.3.2 Change in surface downwelling shortwave radiation

The projected change in incoming shortwave radiation reaching the land surface over West Africa for RCP4.5 scenario and 1.5°C global warming is shown in the Fig 11(a) – 11(h) and 2°C global warming in the Fig 11(i) – 11(p). In 1.5 and 2°C global warming, the projected changes in downwelling shortwave solar radiation for RCP4.5 scenario exhibits no agreement about the downwelling shortwave radiation change over West Africa region. For both global warming level, the spatial distribution in the projected change downwelling shortwave radiation varies among the

RCM members. The CLMcom members (CNRM and MPI) project generally an increase in downwelling shortwave radiation in both global warming. The core of that increase in located in the Sahel region and in some parts of the Savannah area. Moreover, the increase is more important in the 2 °C (up to 4 W/m$^2$) than 1.5 °C global warming level (up to 2 W/m$^2$). Nonetheless, the CLMcom diving by HadGEM shows a decrease in downwelling shortwave radiation in most of the countries in West Africa for 1.5 °C global warming level (0-2 W/m$^2$) and exhibits an increase over the Sahel region and a decrease in the Savannah and Guinean zones (0-2 W/m$^2$) in the 2 °C global warming level. As for the RCA driving by HadGEM, it projects a decrease in downwelling shortwave radiation over West Africa for both global warming level. However, the ensemble mean CLMcom shows an increase in downwelling shortwave radiation with significant change in the Sahel and RCA ensemble mean projects a decrease in downwelling shortwave radiation magnitude over West Africa.

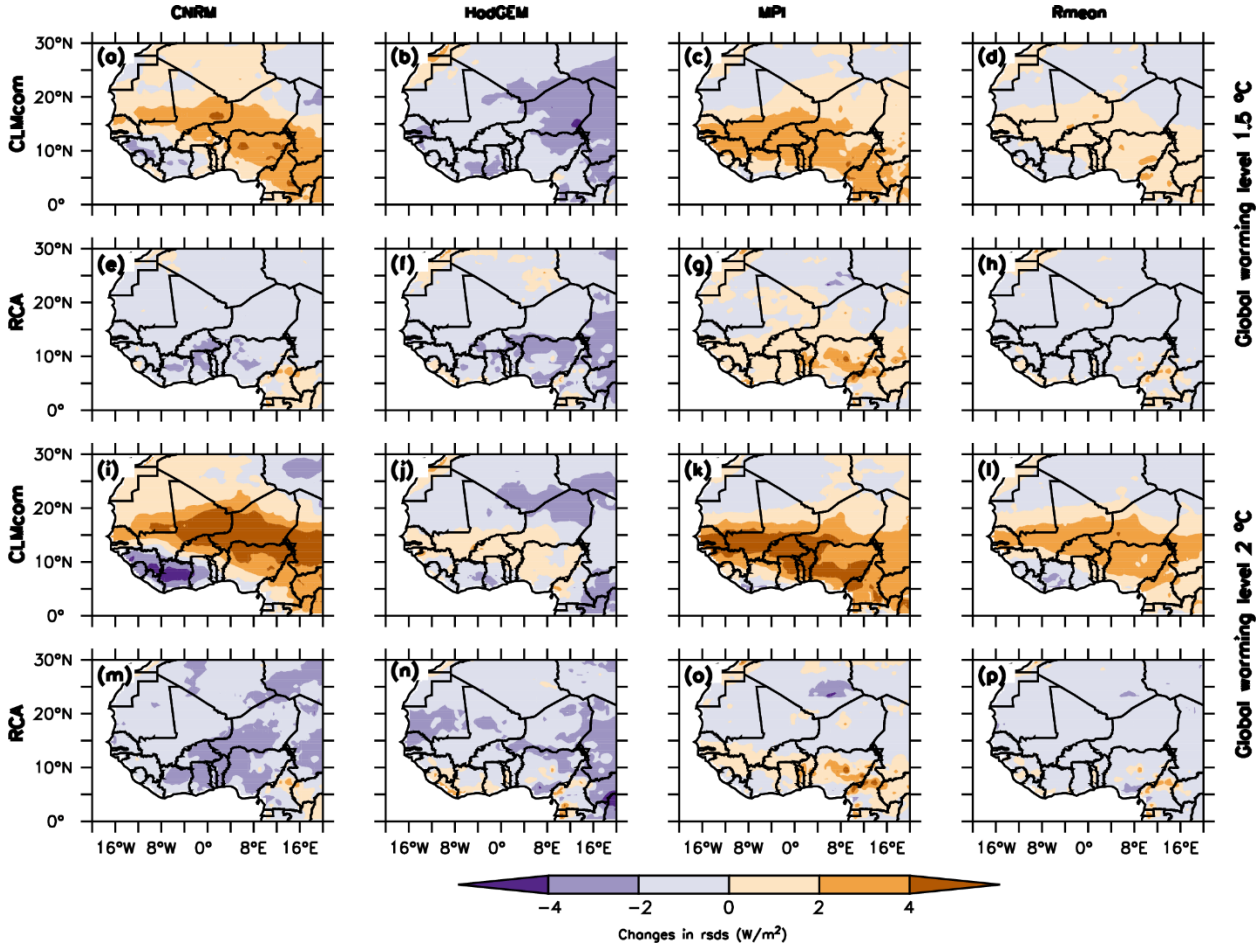


**Figure.11** *Spatial distribution of RCM members and their ensemble mean of the change in surface downwelling shortwave radiation over West Africa of 1.5 and 2 global warming level under RCP 4.5.*

50% of Ouagadougou daily data show no variation in RSDS in all the RCMs projection for both global warming (Figure 12). However, from 25% to 75% of data, the CLMcom members predicts more wide spread in the daily downwelling shortwave radiation than the RCA members. The CLMcom members show for both global warming level the similar box spread. 25 % of the daily data project a decrease about 50 W/m$^2$ and 75% exhibits an increase of the same magnitude for both global warming. Similar observation occurs for the RCA members but with roughly 20 W/m$^2$ for both trend. The ensemble mean of CLMcom for both warming shows large spread of daily shortwave radiation than RCA ensemble mean spread in Ouagadougou. Also, some models project a variation in daily radiation magnitude. Thus the magnitude of radiation could reach the maximum value of 300 W/m$^2$ as RCA-CNRM daily change predict it and the minimum value of -300 W/m$^2$ as RCA-MPI daily change predict in 1.5°C global warming.

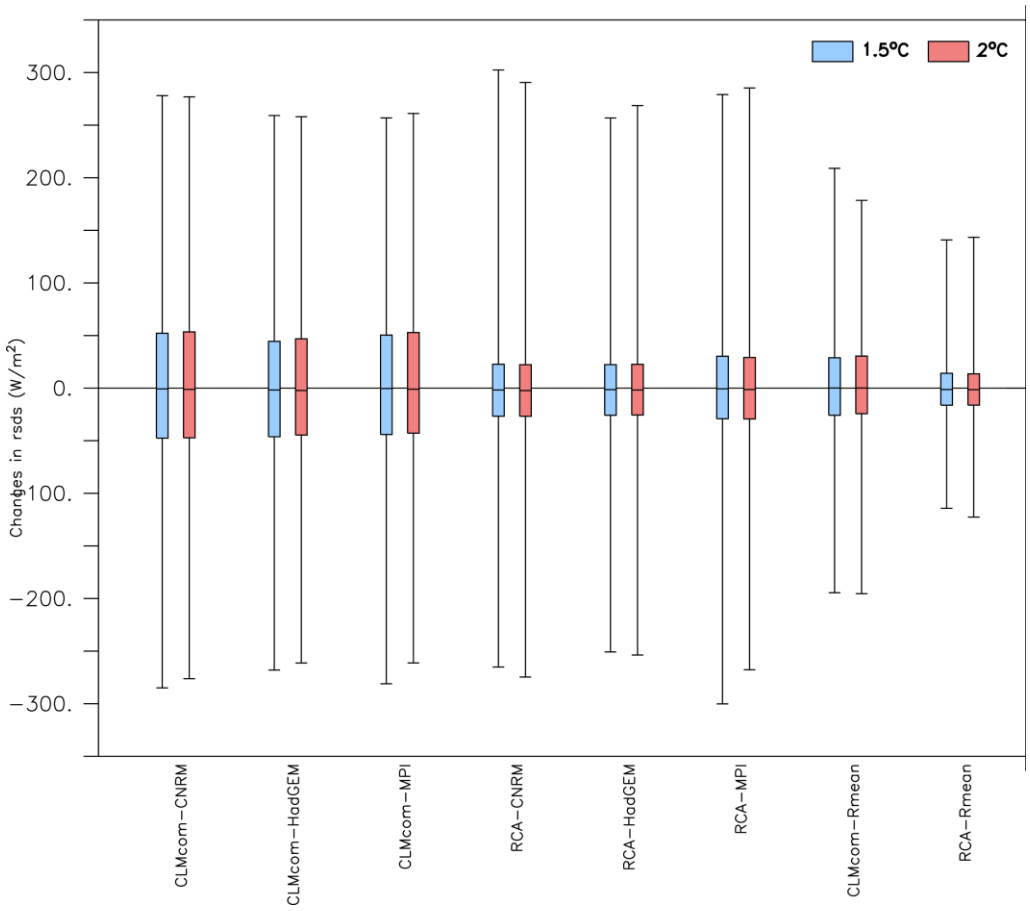


**Figure.12** *Boxplot of the change in surface downwelling shortwave radiation of RCM members and their ensemble mean for 1.5 and 2 ºC global warming level over Ouagadougou under RCP 4.5.*

### 4.3.3 Change in surface wind speed

Under RCP 4.5, the projected change in surface wind is shown in the Figure 13(a) – 13(h) for the 1.5 °C global warming level and the Figure 13(i) – 13(p) for the 2 °C global warming scenario. Most of the RCM members and their ensemble mean exhibit an increase of surface wind over the Sahel region and a decrease over the Guinean zone for both global warming level. The CLMcom members and the ensemble mean do so. However, the decrease is more in CNRM member over the South-Western part and the increase is higher in the HadGEM member over the Sahel for the 1.5 °C global warming level. The 2 °C global warming projects generally an increase of surface wind over the Sahel region and a decrease in most of the Guinean zone for the CLMcom members. Furthermore, the RCA driving by HadGEM and MPI project similar outcome where there is an increase of surface wind over the Sahel region and decrease over the Guinean zone for both global warming level. Nonetheless, the RCA driven by CNRM project, chiefly a decrease of surface wind over West Africa for 1.5 and 2°C global warming level. The spatial distribution of the projected change in surface wind over West Africa for 1.5 °C global warming level is the same with the 2 °C global warming level for both RCM member ensemble mean. The increase is more pronounce in 2 °C global warming level rather than the 1.5 °C global warming level. Nevertheless, the projected change in surface wind over West Africa for both global warming level is negligible where the change varies from -0.1 to 0.1 m/s.

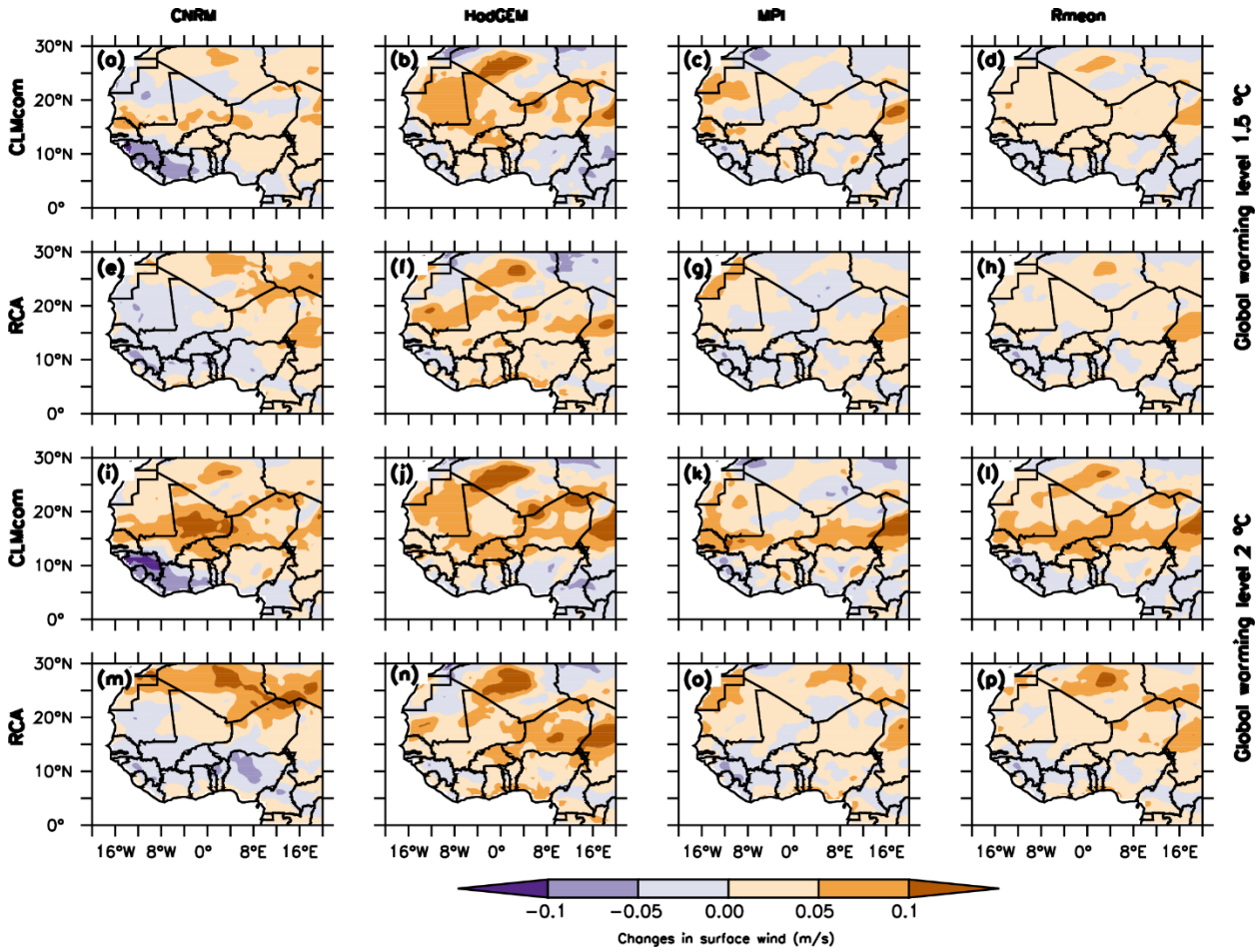


**Figure.13** *Spatial distribution of RCM members and their ensemble mean of the change in surface wind speed over West Africa of 1.5 and 2 global warming level under RCP 4.5.*

For both global warming level, the RCM members project a daily variation of surface wind in Ouagadougou. However, 50% of the daily data from each RCM members and their ensemble mean project no variation of surface wind in Ouagadougou for both global warming level. Although, 75% and 25 % of the daily data of the RCM members exhibit an increase of 1 m/s and a decrease of 1 m/s respectively for both global warming level. Moreover, the box spread (25% to 50%) of each RCM member shows similar variation of daily surface wind in Ouagadougou for both global warming level. The box spread of their ensemble mean is less than the RCM members. That spread goes from -0.5 to 0.5 m/s. Besides, some RCM members project days where the wind speed will change dramatically. For instance, under 2 °C global warming level, the CLMcom driving by CNRM project a decrease of surface wind of about 9 m/s and an increase which is roughly 8.5 m/s. The 1.5 °C global warming level project a maximum value for the wind speed up to 12 m/s. But

the CLMcom ensemble mean project an increase of maximum value up to 4 m/s both global warming level, whereas the RCA ensemble mean shows a maximum value less than 4 m/s. Both ensemble mean and global warming level, they project a minimum value less than 3 m/s.

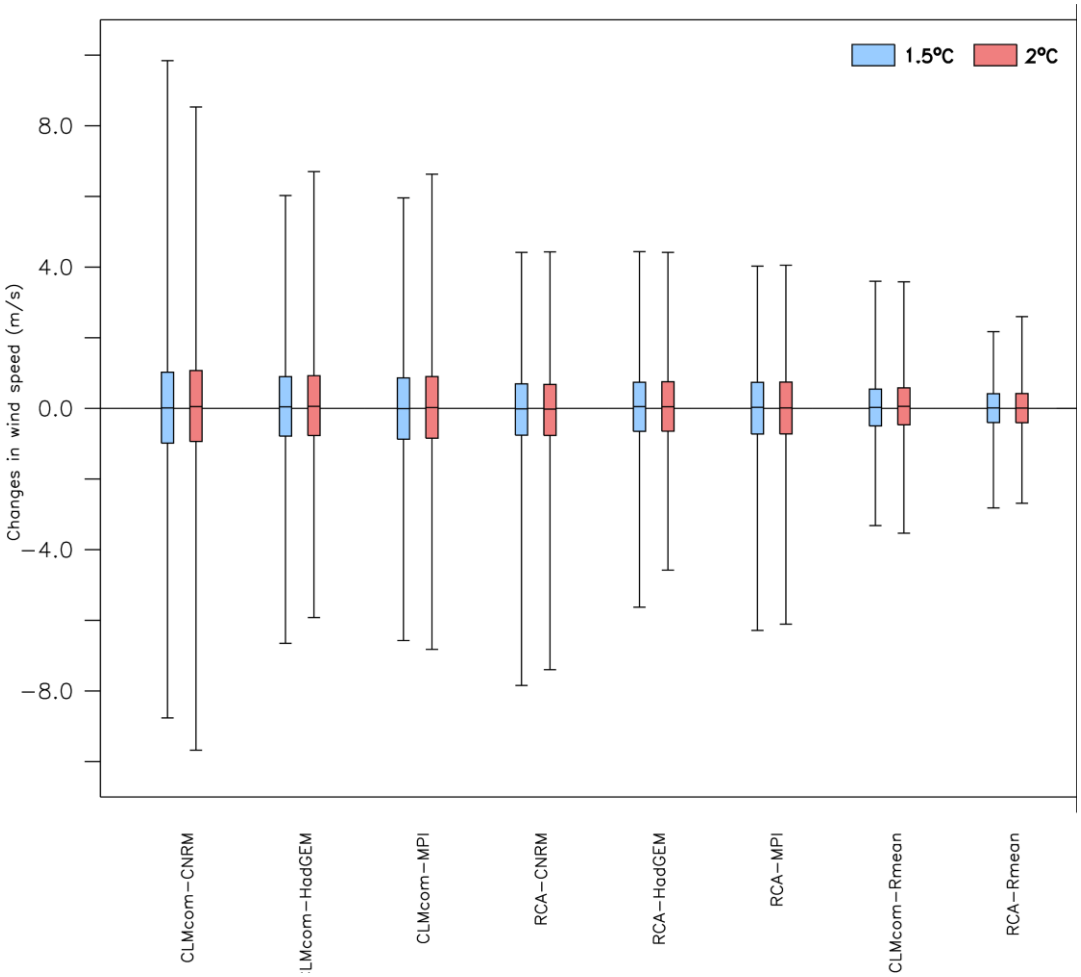


**Figure.14** *Boxplot of the change in surface wind speed of RCM members and their ensemble mean for 1.5 and 2 ºC global warming level over Ouagadougou under RCP 4.5.*

### 4.3.4 Photovoltaic Potential

The future change of Photovoltaic potential over West Africa for the 1.5 °C global warming is shown in Fig 15(a)-15(h) and the 2 °C global warming in Fig 15(i)-15(p) from the RCM members and their ensemble mean. There is no agreement on the change of PV potential over West Africa in both global warming level. Some RCM members project an increase and a decrease of PV potential over the subcontinent. However, the spatial distribution of each RCM (CLMcom and RCA) shows a different change of PV potential over West Africa. The CNRM driven by CLMcom project generally an increase of PV potential over West Africa (up to 20 °N) except in Cote D'Ivoire and Guinea where there is a decrease under 1.5 °C global warming level. Under 2 °C global warming level that increase and decrease are more pronounced than the 1.5 °C global warming level. In addition, the decrease could reach some part of Ghana. The core of the increase is chiefly located in the Sahel region. In contrast, the CLMcom driving by MPI projects an increase of PV potential over West Africa (up to 20 °N) with the core of the increase in the Sahel region. Again, the 2 °C global warming level shows more increase than the 1.5 °C global warming level. Another RCM member; the HadGEM driving by CLMcom predicts a decrease in the PV potential over West Africa under 1.5 °C global warming level. Nonetheless, the 2 °C global warming level shows an increase over the Sahel zone and some parts of the Savannah area. As for the RCA members (CNRM and HadGEM) exhibit a decrease in PV potential over West Africa for both global warming level. The MPI from that RCM project an increase in the Guinean region and in some parts of the Sahel area for the 1.5 ° C global warming level while in the 2 °C global warming level, it projects a decrease in PV potential in the Guinean zone and an increase in the Savannah and Sahel region. In general, the RCA ensemble mean projects over West Africa a decrease in PV potential for both global warming level. The CLMcom ensemble mean projects an increase in PV potential most in the Sahel region in both global warming level.

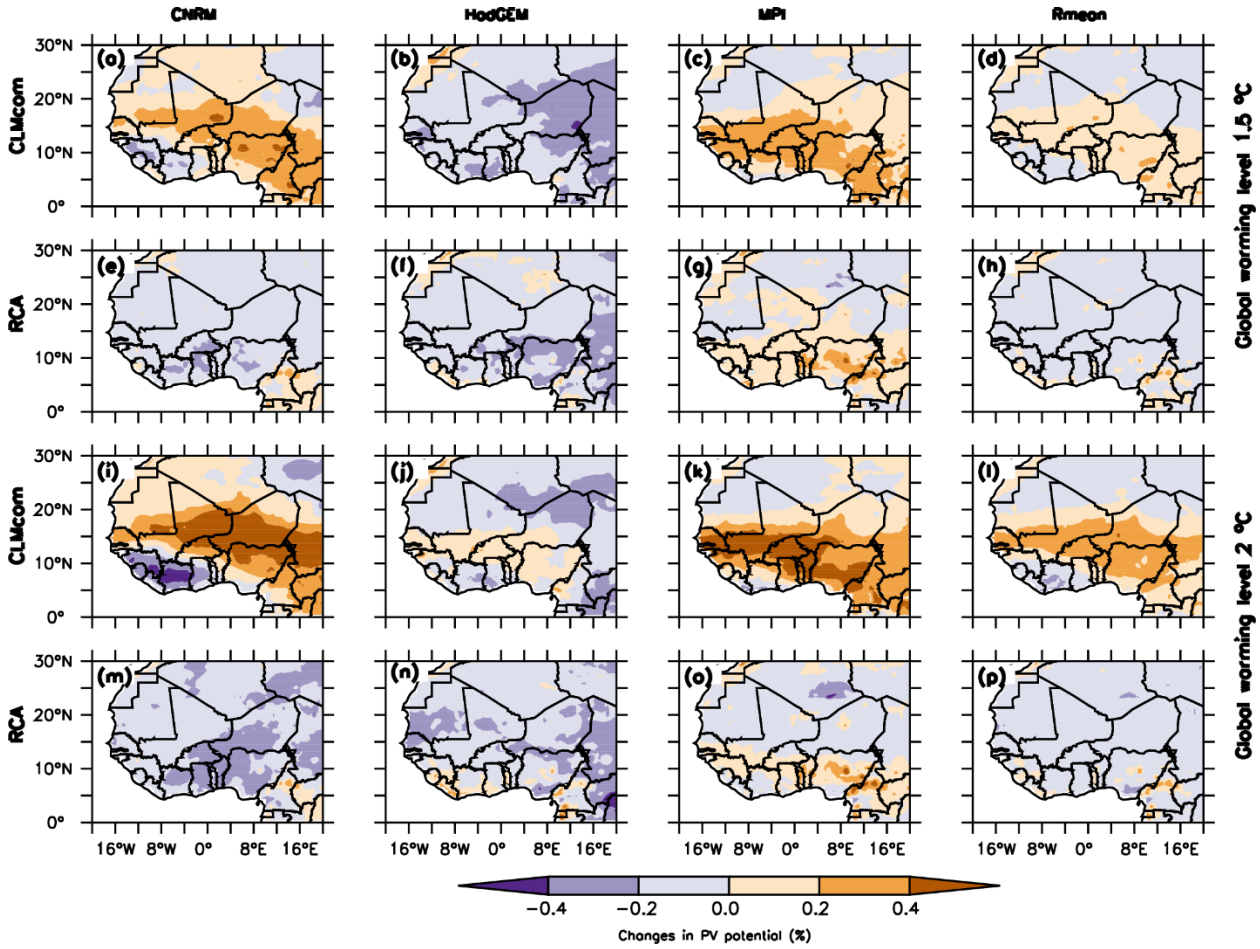


**Figure.15** *Spatial distribution of RCM members and their ensemble mean of the change in PV potential over West Africa of 1.5 and 2 global warming level under RCP 4.5.*

The daily change in PV potential in Ouagadougou for both global warming level in the Figure 16 exhibits a variation for each RCM members. There is an agreement of the variation of the box spread among RCMs but differ from each RCMs. However, there is no change in the PV potential for both global warming in Ouagadougou. 50 % of the daily data from each RCM members do so. As shown in the figure, the CLMcom members show the same box spread for both global warming level. The box spread of the CLMcom members is higher than the one of RCA members. In both global warming level, 75% of the CLMcom members project an increase (5%) in daily PV potential and 25 % predicts a decrease of 5 % of the daily PV potential in Ouagadougou. However, the RCA members projects an increase of 2 % and a decrease of 2 % for 75 % and 25% of the daily PV potential respectively. The CLMcom ensemble mean project similar magnitude in terms

of 75 % and 25 % of the daily variation of PV potential. As for the RCA ensemble mean it is roughly 1 % of the daily in PV potential.

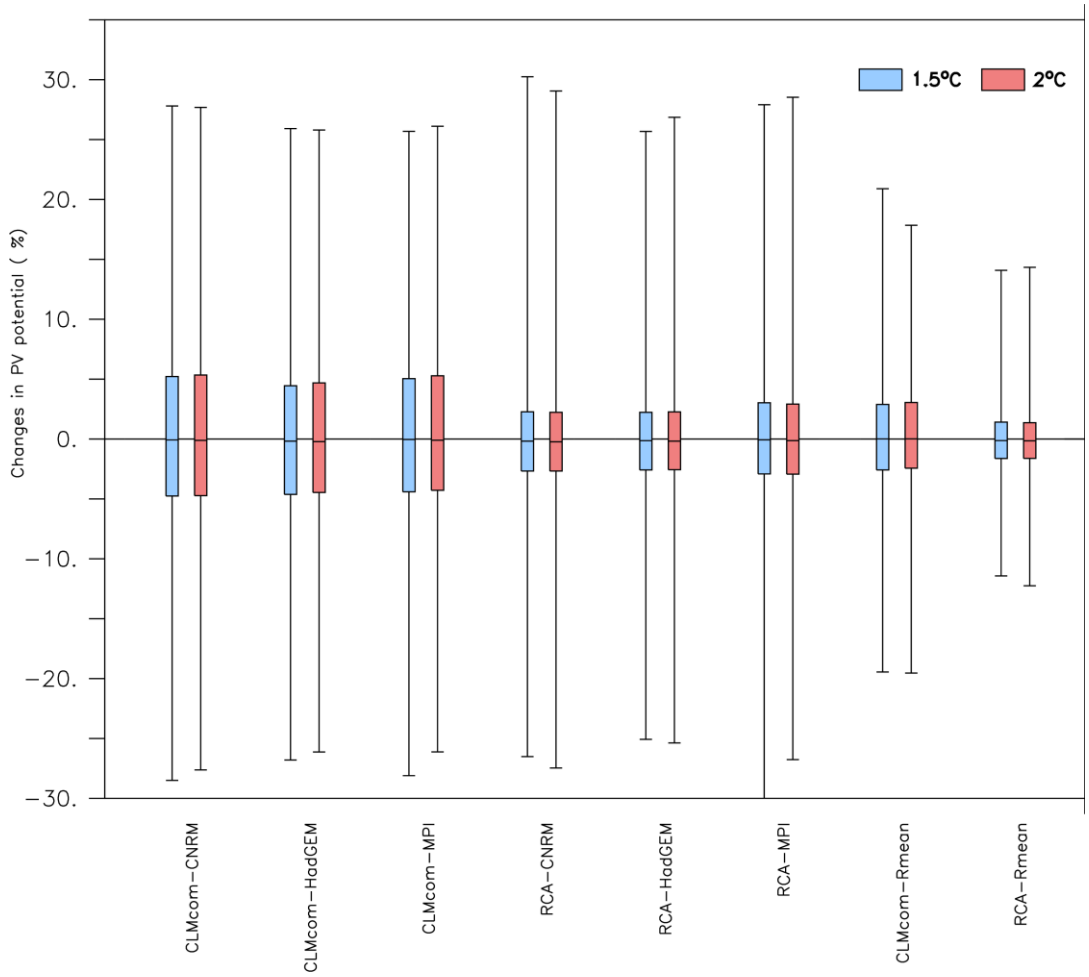


**Figure.16** *Boxplot of the change in PV potential of RCM members and their ensemble mean for 1.5 and 2 ºC global warming level over Ouagadougou under RCP 4.5.*

## 4.4 Climate change scenario under RCP 8.5

### 4.4.1 Change in surface air temperature

The figure 17(a)-17(h) shows the change in surface air temperature of RCM members for the 1.5 ° C global warming level and the Figure 17(i)-17(p) for the 2 ° C global warming level under RCP 8.5 climate change scenarios. There is an agreement of the RCM members and their ensemble mean in the increase in surface air temperature over West Africa for both global warming under

RCP 8.5 climate change scenario. Both climate change scenario (RCP 4.5 and RCP 8.5) and global warming level (1.5 ° C and 2 ° C) agree with the increase in air temperature over the subcontinent. The warming is more in the Sahel region than the Savannah and Guinea regions. However, the warming in RCP 8.5 is more spread than the RCP 4.5. For instance, the HadGEM driven by CLMcom shows that the core of the warming is more spread in terms of spatial distribution under RCP 8.5 than the RCP 4.5 for the 1.5 °C and 2 °C global warming level. This spread even reaches the Savannah area. Same result is found with the MPI driven by CLMcom under 1.5 °C global warming level. Nonetheless, the overall average warming of the subcontinent for 2 °C global warming level under RCP 8.5 exhibits less warming than the RCP 4.5 with the same RCM member. The opposite result appears in the different RCM (RCA) with the same global warming level. The CNRM driven by CLMcom and RCA project almost the same magnitude of warming over West Africa as in RCP 4.5 climate change scenario under 1.5 global warming level. On the other hand, the core of the spatial distribution of the CLMcom driven by CNRM covers the whole Benin, Togo and some southern part of Nigeria under 2 °C global warming level while under RCP 4.5, the boundary of the warming core is limited above 12 ° N and from 16W to 16° E. The ensemble mean generally projects higher warming under RCP 8.5 than RCP 4.5 for both global warming levels.

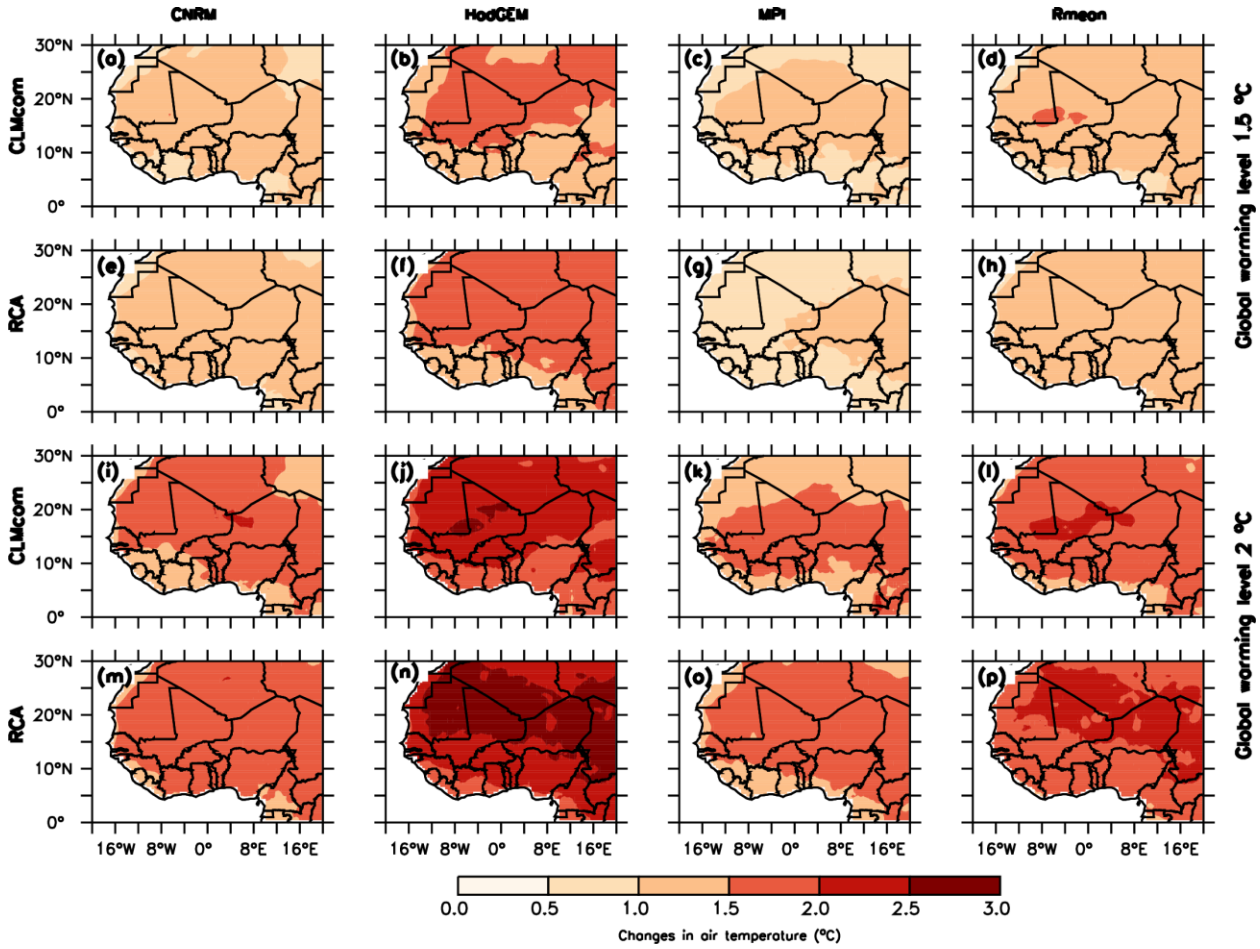


**Figure.17** *Spatial distribution of RCM members and their ensemble mean of the change in the surface air temperature over West Africa of 1.5 and 2 global warming level under RCP 8.5.*

All the RCM members agree on the increase of daily surface air temperature in Ouagadougou (Figure 18). In both global warming, 50% of the daily data of each RCM members project that increase. The magnitude of 50% of the daily data is higher in 2 °C global warming level than the 1.5 °C. There is an agreement with the one found in the RCP 4.5 climate change scenario. However, the change in the future projection in surface air temperature exhibits a different magnitude for both RCPs and global warming levels. To point out, 50% of the daily data for the CLMcom driving by MPI for the 1.5 °C global warming level dropped under RCP 8.5 compared to the RCP 4.5. However, 25% and 75% of the data show an increase under RCP 8.5. Nonetheless, all the remaining RCM members exhibit no variation in the change of the surface air temperature for both global warming level in Ouagadougou. The CLMcom ensemble mean shows slight change under RCP 8.5 for the 1.5 °C global warming level.

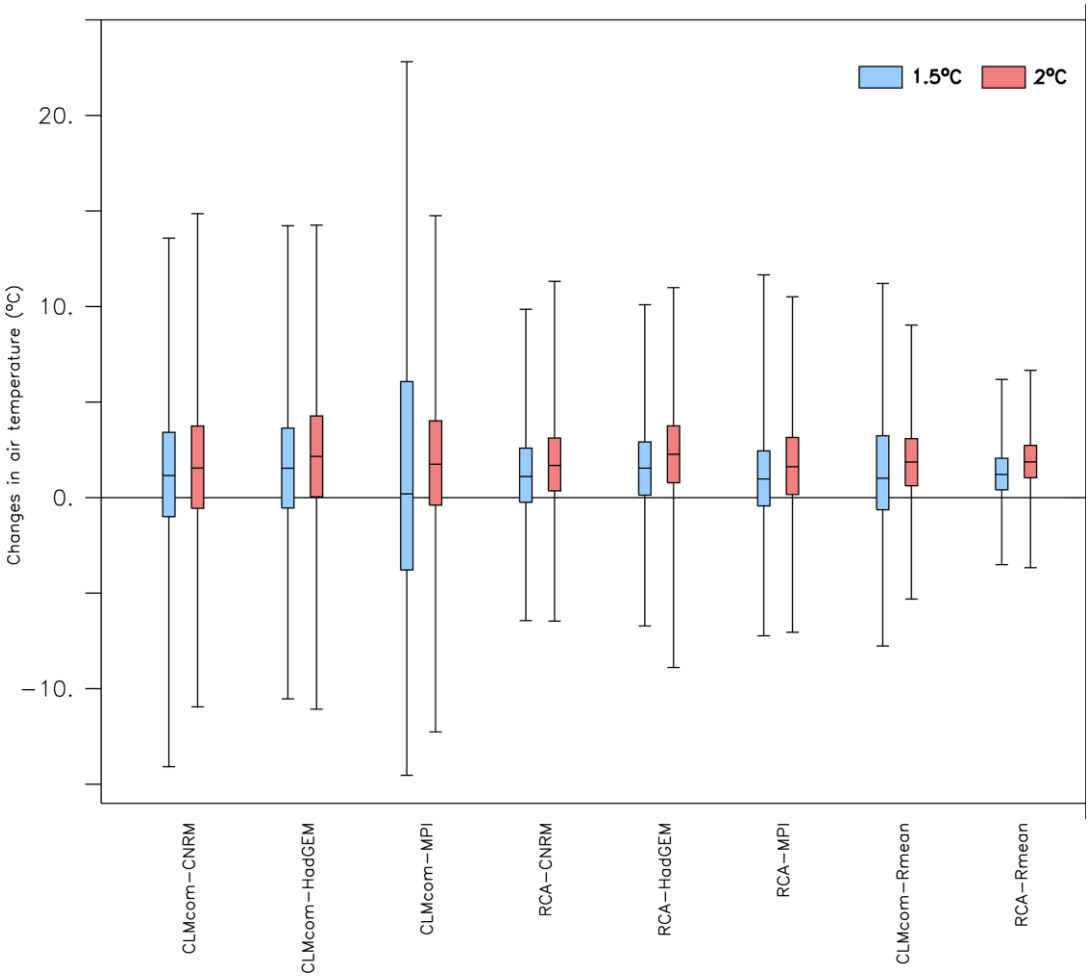


**Figure 18** *Boxplot of the change in the surface air temperature of RCM members and their ensemble mean for 1.5 and 2 ºC global warming level over Ouagadougou under RCP 8.5.*

### 4.4.2 Change in surface downwelling shortwave radiation

For both global warming level and RCPs, there is a similar spatial distribution in the change of RSDS over West Africa. In other words, Each RCM member under RCP 8.5 is able to replicate the spatial distribution the change of RSDS over West Africa correspondingly to the RCP 4.5. There is an agreement of the CLMcom driven by CNRM in the increase of RSDS over the Sahel zone and over the South-Eastern part of the Guinean zone under RCP 8.5 (Figure 19). Note, the increase in 2 °C global warming level is higher than the 1.5 °C global warming level. Furthermore, the magnitude of the increase in the change in RSDS over West Africa under RCP 8.5 exhibits higher changes than the RCP 4.5 for both global warming level. Nonetheless, the MPI driven by

CLMcom shows the increase in RSDS over the Sahel region under RCP 8.5 is less than the RCP 4.5 in both global warming level. Identically, the RCA driving by MPI simulates the same observation. While the CLMcom MPI shows an increase over the south-Western part over West Africa under RCP 8.5, the RCP 4.5 generally exhibited a decrease over West Africa for the 1.5 °C global warming level. In addition, the overall average over the three regions over West Africa projects less increase under RCP 8.5 compared to the RCP 4.5 for the 2 °C global warming level. Different from that, the RCA driving by HadGEM under RCP 8.5 and 2 °C global warming level predicts generally a decrease of RSDS with magnitude superior to the RCP 4.5 over West Africa. While the HadGEM driven by CLMcom projects a slight decrease under RCP 8.5 over the Sahel zone, the RCP 4.5 predicts a slight increase over the same domain. For both global warming level, the RCM ensemble mean project more increase and less decrease of RSDS over West Africa under RCP 8.5 in comparison to RCP 4.5.

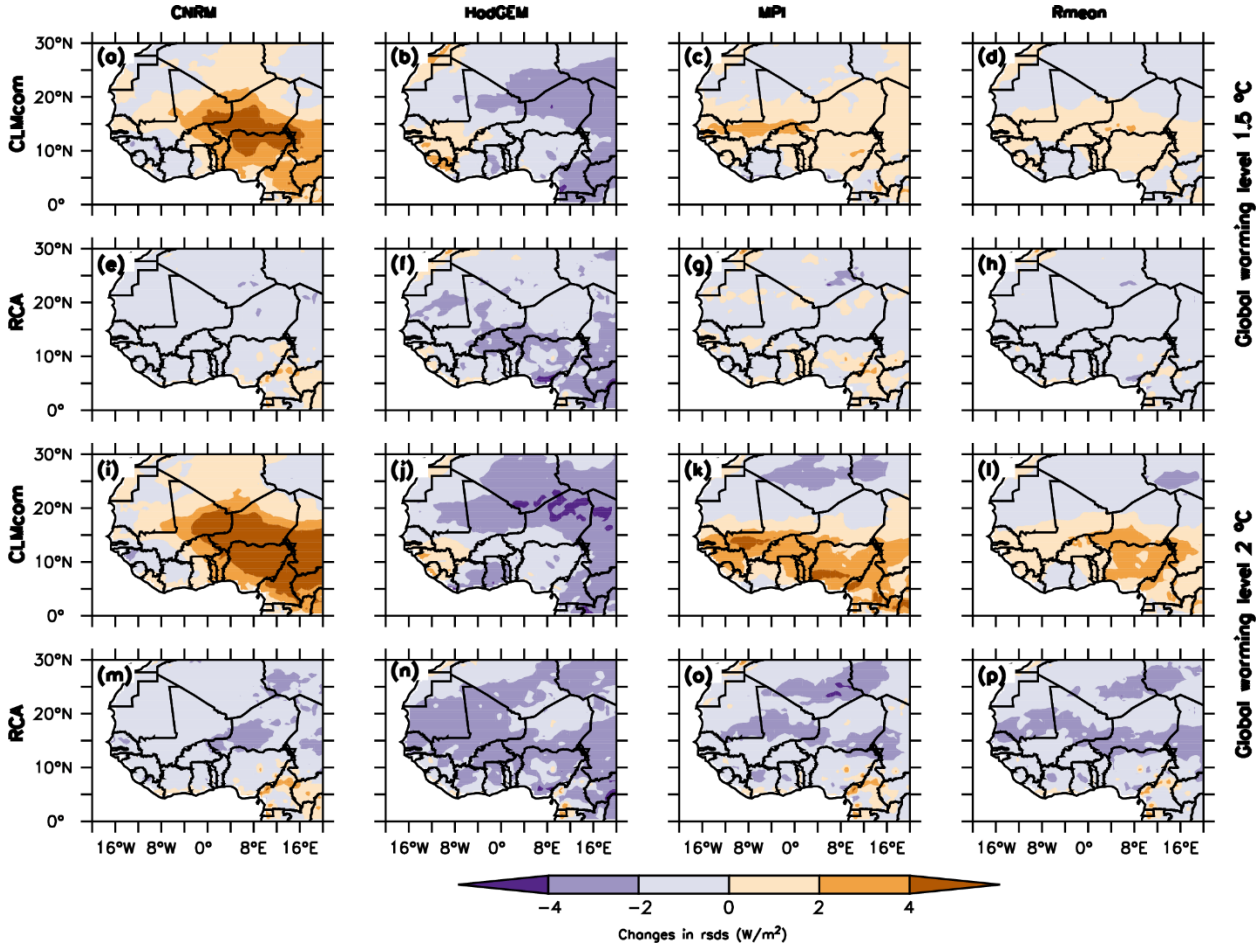


**Figure.19** *Spatial distribution of RCM members and their ensemble mean of the change in the surface downwelling shortwave radiation over West Africa of 1.5 and 2 global warming level under RCP 8.5.*

There is a similarity between the RCP 8.5 and RCP 4.5 climate change scenario in the future change of RSDS in Ouagadougou for both global warming level. However, 50% of the daily RSDS in Ouagadougou projects, there will not be a variation of the RSDS for all the RCM members and both global warming level except the CLMcom driving by MPI at 1.5 °C global warming level where 50% of the daily data predicts an increase in RSDS about 10 W/m2 (Figure 20). Similar to the 75% of the daily data where the RSDS may increase more than 50 W/m2. On the other hand, the minimum and the maximum value of each RCM member under RCP 8.5 are different from the RCP 4.5. The RCA ensemble mean presents the same variation of the box spread as the RCP 4.5 for both global warming levels. The CLMcom ensemble mean for 2 °C global warming level does so while the box spread under RCP 8.5 is higher than the RCP 4.5 for the 1.5 °C global warming level.

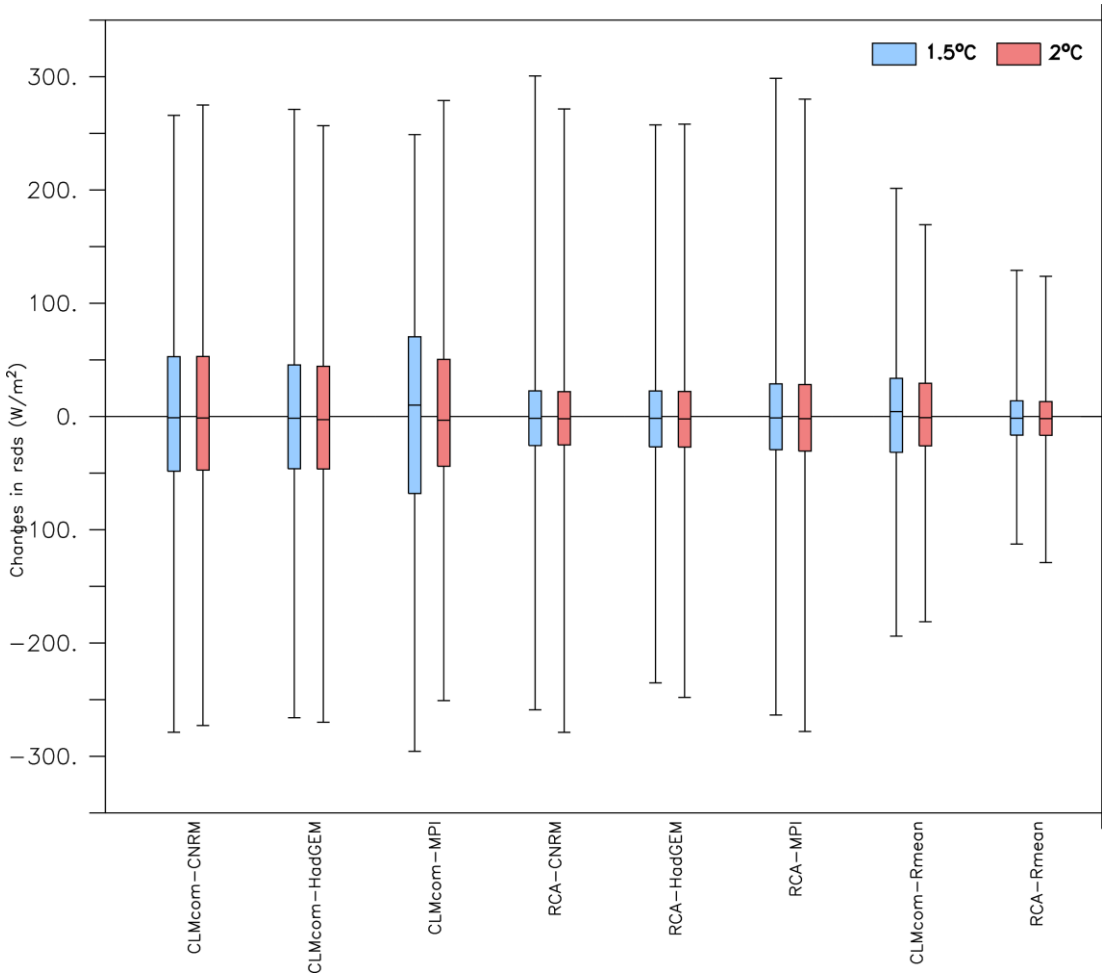


**Figure.20** *Boxplot of the change in the surface downwelling shortwave radiation of RCM members and their ensemble mean for 1.5 and 2 ºC global warming level over Ouagadougou under RCP 8.5.*

### 4.4.3 Change is surface wind speed

The RCM members project an increase in surface wind over the Sahel region and decrease over the Guinean zone under RCP 8.5 for both global warming level. This corroborates with the one find in RCP 4.5 for both global warming level. The Sahel region may know less increase and decrease of surface wind under RCP 8.5 (Figure 21) compared to RCP 4.5. However, the magnitude of each RCM member under RCP 8.5 differs with the magnitude in the change of surface wind under RCP 4.5. For instance, the magnitude of the decrease in CLMcom driving by CNRM under RCP 8.5 is less in comparison to RCP 4.5 for both global warming level especially in Cote D'ivoire and Guinea. Over the Sahel region, similar observation may occur in the change of surface wind speed. In both RCMs (CLMcom and RCA) and both global warming level, the HadGEM projects an increase in surface wind under RCP 8.5 over the Guinean zone which is in contrast with the one under RCP 4.5 where it generally predicts a decrease in surface wind over the same zone. The spatial distribution of MPI in the change of surface wind in both RCMs and both global warming level under RCP 8.5 much the same with the one in RCP 4.5. Though, the CLMcom in 2 °C global warming level exhibits higher increase in the Sahel area under RCP 8.5 than RCP 4.5. The projection in the change in surface wind over West Africa of the RCM ensemble mean project similar pattern with the RCP 4.5 for both global warming except the RCA ensemble mean in 1.5 °C global warming level where the RCA under RCP 8.5 predicts an increase, the RCP 4.5 may have a decrease over the Sahel region. Nevertheless, this change of each ensemble member and in both global warming, the change is not significant in term of magnitude of wind speed (0.1 to 0.1 m/s).

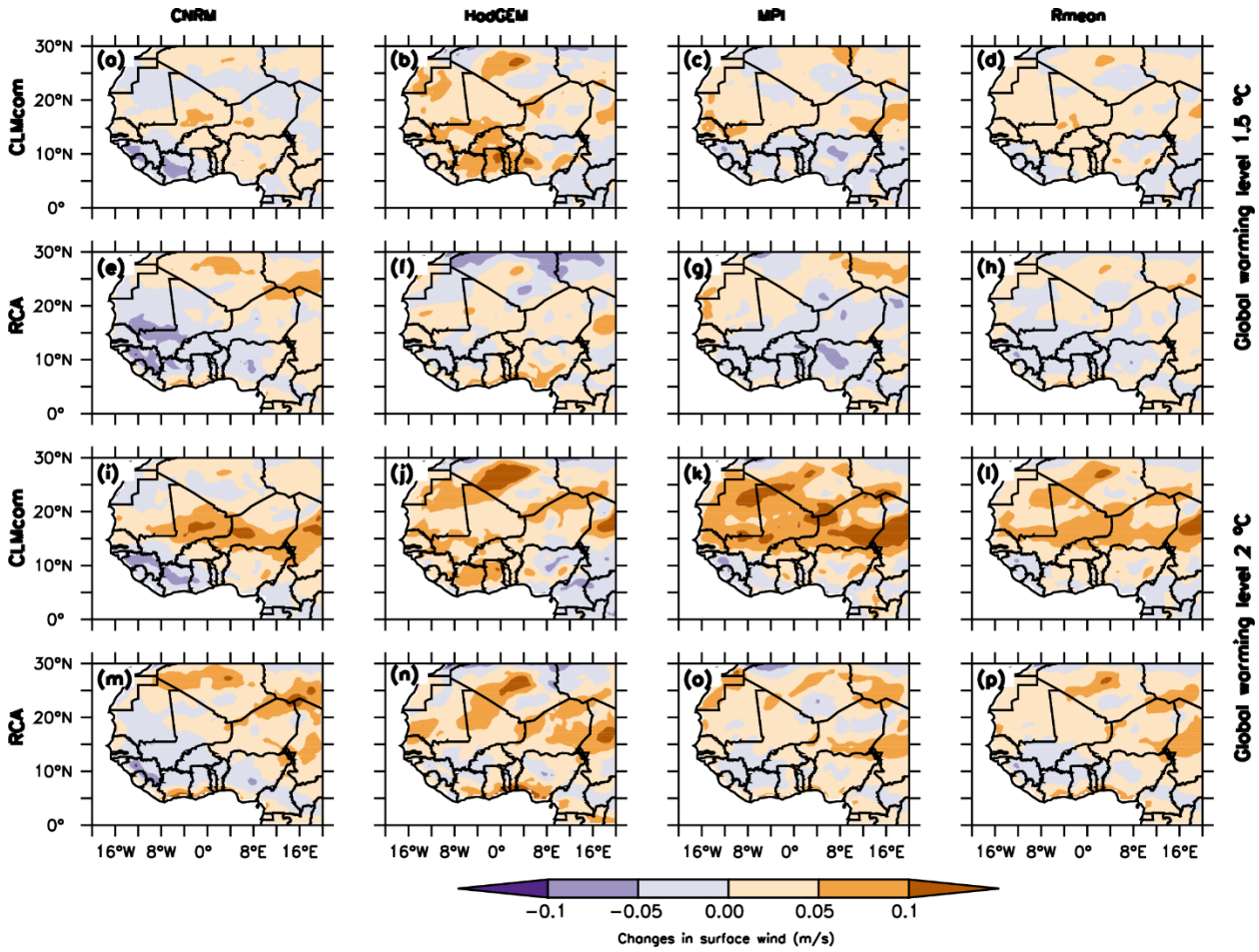


***Figure 21*** *Spatial distribution of RCM members and their ensemble mean of the change in the surface wind speed over West Africa of 1.5 and 2 global warming level under RCP 8.5.*

There is no variation in the change of surface wind in Ouagadougou of the 50% daily data of the RCM members on both global warming level (Figure 22). There are 75% of the daily of the RMC members predict an increase and 25% project a decrease of wind speed in both global warming level. Both RCPs in both global warming level have similar variation in the change of surface wind speed in Ouagadougou. However, the maximum and minimum from each RCM members and their ensemble mean differ from the RCPs. Furthermore, the MPI driven by CLMcom show more decrease in terms of 25% of the daily data in comparison with the RCP 4.5.

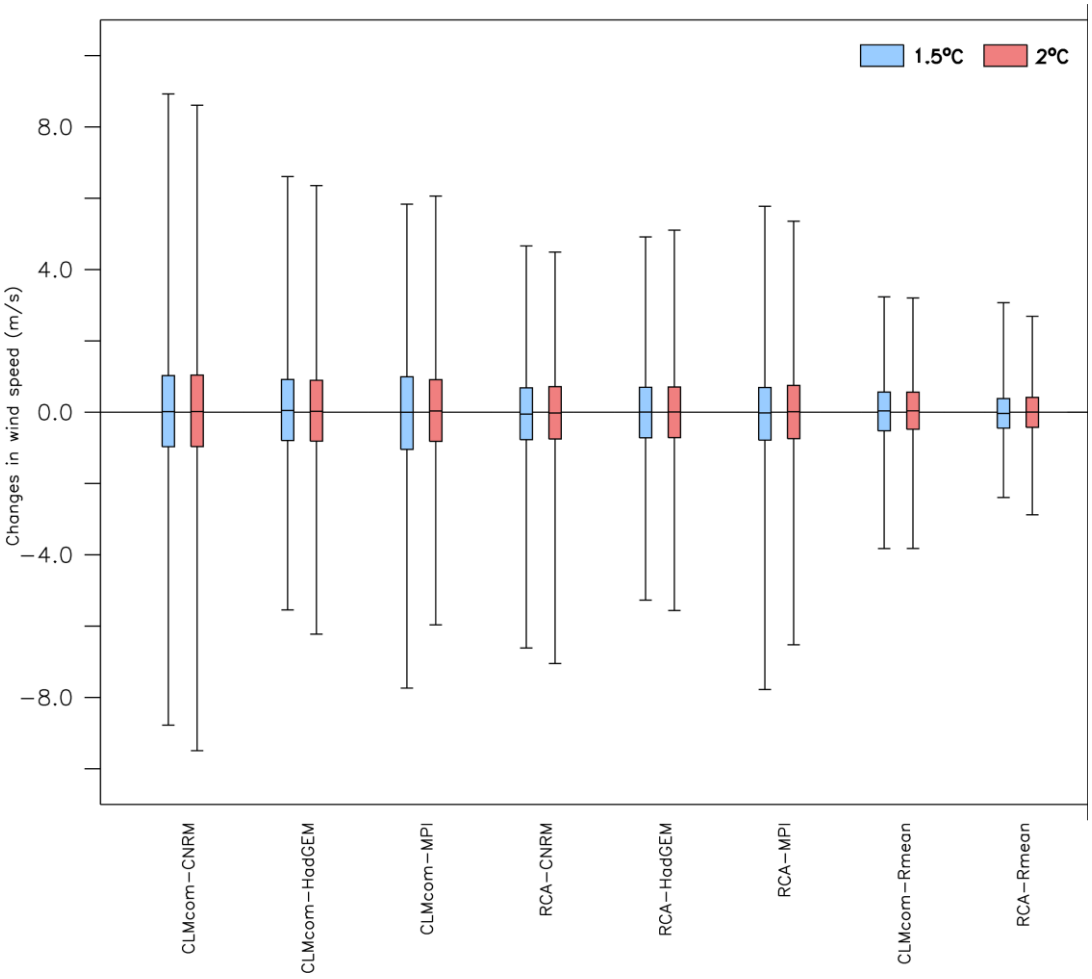


**Figure.22** *Boxplot of the change in the surface wind speed of RCM members and their ensemble mean for 1.5 and 2 ºC global warming level over Ouagadougou under RCP 8.5.*

### 4.4.4 Change in the PV potential

The corresponding RCM members between both RCPs in both global warming level show the similar spatial distribution in the change of PV potential over West Africa. Yet, there is a discrepancy between the corresponding RCM members about the location of increase and decrease in PV potential over West Africa for both global warming levels. Furthermore, they show differences in the magnitude of the change of PV potential. For example, while the CLMcom driven by HadGEM project an increase in PV potential for 1.5 °C global warming level around Liberia, Guinea and Serra-Leona under RCP 8.5, the RCP 4.5 a decrease in the change of PV potential. In contrast, it predicts an increase, whereas under RCP 4.5 it predicts a decrease for 2 °C global warming. Moreover, there is a discrepancy over the Sahel region between both RCPs in

the 2 °C global warming level. The RCP 8.5 exhibits a decrease while the RCP 4.5 shows an increase. Generally, the HadGEM projects a decrease in PV potential over West Africa under RCP 8.5. Nonetheless, the CNRM projects similar pattern as the RCP 4.5 for both global warming levels. The magnitude of the increase is higher than the one found in RCP 4.5 and the decrease in the change in PV potential is less than the RCP 4.5. As for the MPI, the Sahel zone may have less increase in PV potential under RCP 8.5 compared to the RCP 4.5.

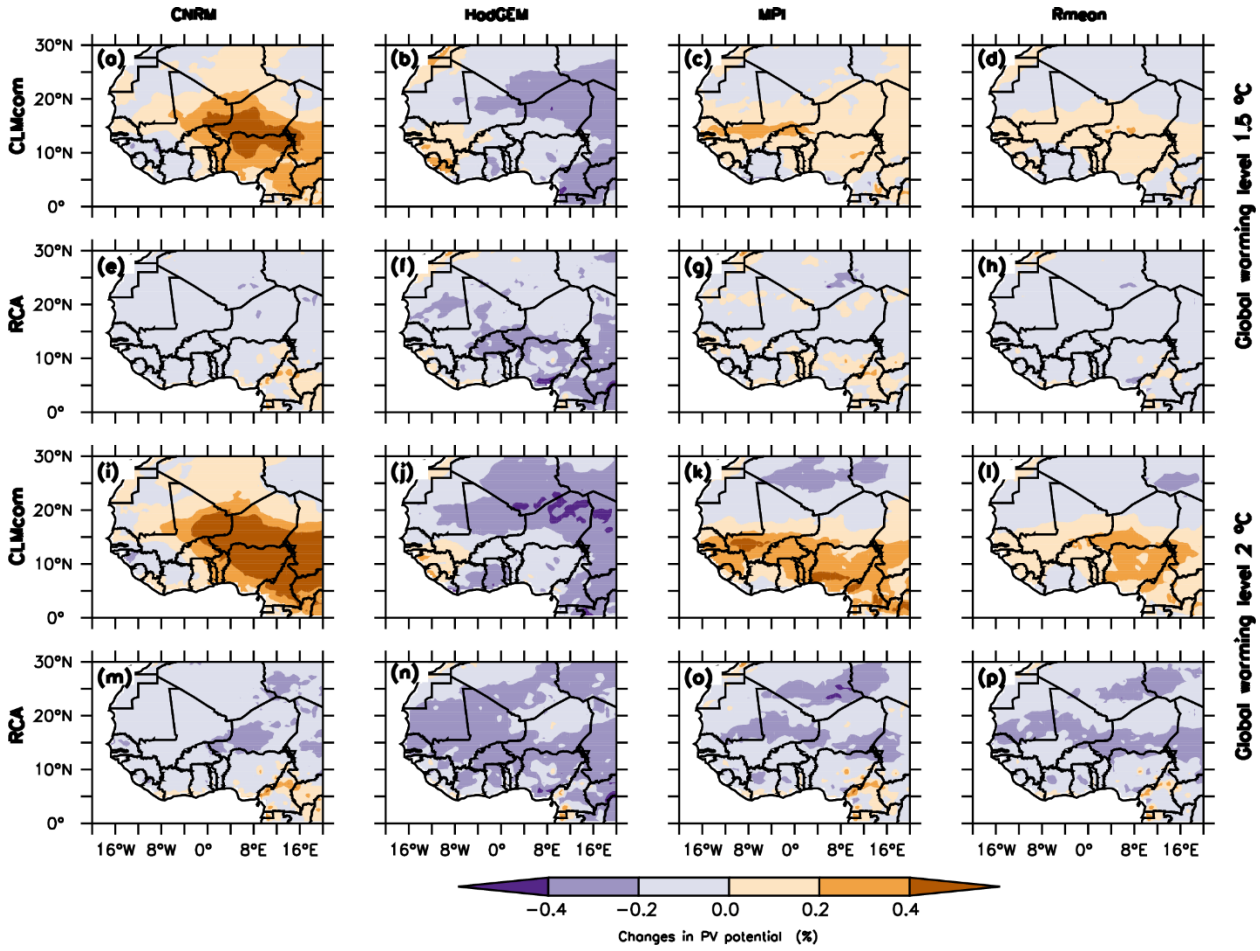


***Figure 23*** *Spatial distribution of RCM members and their ensemble mean of the change in the surface PV potential over West Africa of 1.5 and 2 global warming level under RCP 8.5.*

Most of the RCM members of 50% of the daily data in PV potential projects, there is no variation in the change in PV potential in Ouagadougou in both global warming levels. In other words, 50% of the daily data prediction, there will not an impact of climate change in the PV potential in Ouagadougou. However, 75 % of the daily data of CLMcom-CNRM and CLMcom-HadGEM

project an increase in PV potential of about 5% while 25% says there will be a decrease in PV potential of about 5% for both global warming levels. This agree with the one found under RCP 4.5. However, the CLMcom-MPI in 1.5 °C global warming differs with the one of RCP 4.5. Here, it projects a slight daily variation in the 50% of the daily PV potential. In Contrast, all the RCA members are similar spread in the daily variation of PV potential with the RCP 4.5 for both global warming level.

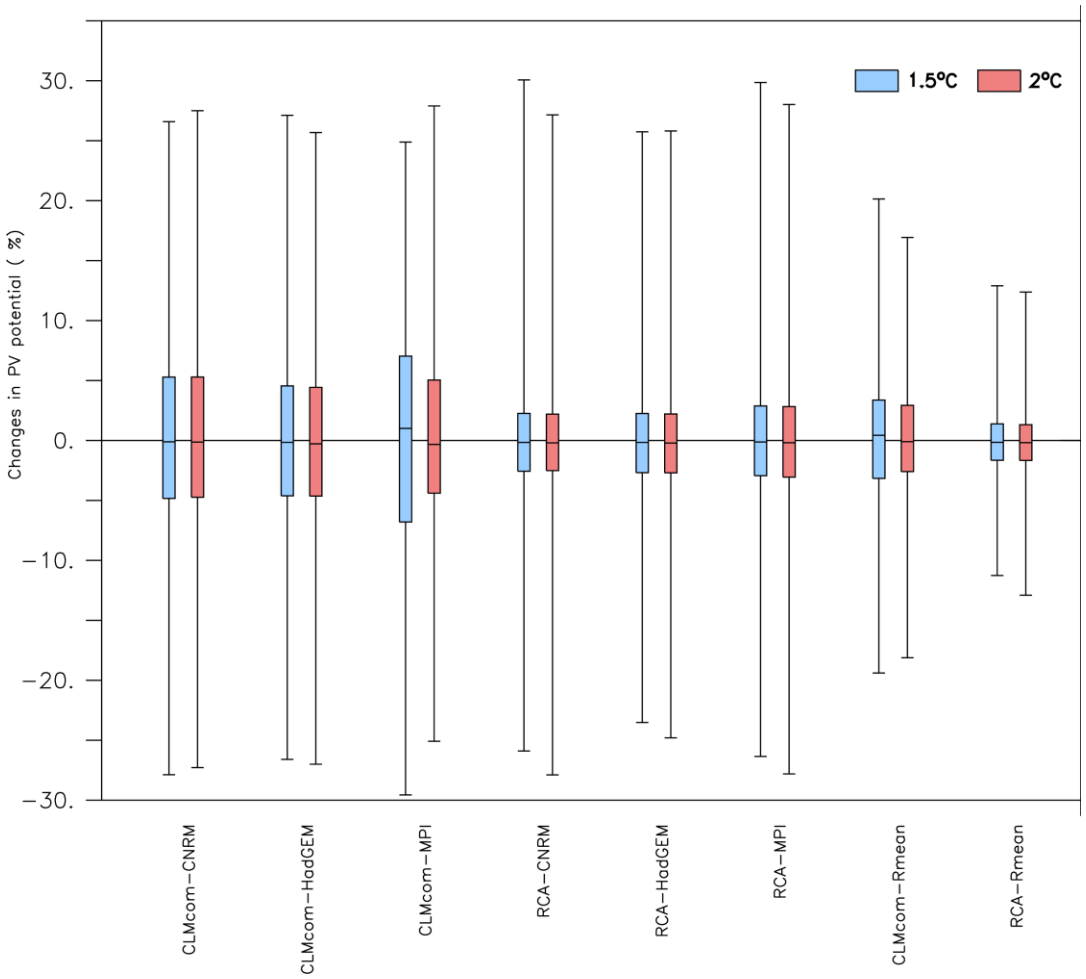


**Figure.23** *Boxplot of the change in the PV potential of RCM members and their ensemble mean for 1.5 and 2 ºC global warming level over Ouagadougou under RCP 8.5.*

## 4.5 Discussion

Renewable energy sources that use natural resources have the potential to provide energy services with zero or almost zero emissions of both air pollutants and greenhouse gases (Demirbas, 2009). Projections are important tools for long-term planning and policy setting. It should be noted that Global Climate Models (GCMs) are the most appropriate tool for addressing future climate change. However, in order to formulate adaptation policies and strategies in response to climate change impacts and vulnerability, reliable climate change information must be resolved at much finer spatial scales and these can be obtained from use a Regional Climate Models (RCMs). These models do provide finer spatial and temporal detail than the GCMs. There is however some uncertainty associated with the development of future climate change scenarios and these typically arise from the assumptions' made with regard to emission scenarios, socioeconomic emissions, GHG concentration projections, climate model projections among others (AMCEN, 2011). (Hu et al., 2016) found that solar panels alone induce regional cooling by converting incoming solar energy to electricity in comparison to the climate without solar panels. We can attribute change in solar power output to change in temperature, solar radiation and location (Crook et al., 2011). Climate change will impact regional patterns of temperature and irradiance, and therefore affect regional PV output. Wind influences the output of PV because forced convection removes heat from the cell and therefore reduces the cell temperature. Dust settling on PV panels is a significant problem in more arid regions.

The impacts of climate change on photovoltaic (PV) output in the fifteen countries of the Economic Community of West African States (ECOWAS) was analyzed by (Dimitri et al., 2016), in their paper used a set of eight climate models, the trends of solar radiation and temperature between 2006–2100 were examined. They show from the eight models a disagreement of solar irradiation trends. Some predict a negative trend of solar irradiation and other a positive trend. This corroborates with our results. There is no agreement between RCM members used in this study on the impact of climate change on RSDS under both RCPs and global warming level over West Africa. Furthermore, there is no agreement on the change in PV potential as well. In other words, at regional scale, the RCM members are not agreeing about the future change in the mean solar radiation and photovoltaic potential. But locally, 50 % of RCM daily simulations over Ouagadougou project no change in incoming solar radiation and PV potential.

Another key point, All RCM members agree about the future warming over West Africa under RCP 4.5 and RCP 8.5 due to the impact of climate change. Nevertheless, this warming will be more accentuated in the Sahel region. This region has been identified by as hotspot of climate change for both RCP 4.5 and RCP 8.5 (Diffenbaugh and Giorgi, 2012) in the late 2030s to early 2040s. Many studies over the region agree with our finding on increase in the climate change under RCP 4.5 and RCP 8.5 of warming (Monerie et al., 2013; Diallo et al., 2012; Sylla et al., 2016).

# Chapter 5

# CONCLUSION AND RECOMMANDATIONS

Most of the electricity production in the world comes from fossil fuels, which have a negative impact on the climate. However, electricity is very crucial to run the socio-economic of any country. We need to produce electricity by taking into account the damage of the environment. Renewable energy sources are environmental friendly and free and lead to sustainable development. Nevertheless, the renewable energy sources are impacted to the climate change and climate variability. There is a need to study the impact of climate change on renewable energy before building large power plant for electricity generation.

West Africa countries commit to electricity mixing especially in the solar energy. Burkina Faso does so. This study projected the impact of climate change on PV potential over West Africa and Ouagadougou under RCP 4.5 and RCP 8.5. This projection is based on the Paris agreement where most of the countries agreed to reduce their emission below the global mean temperature 2 °C. Here, we projected the RSDS, surface wind speed, air temperature and PV potential for 1.5 and 2 °C global warming level. To perform this projection, 6 RCM members from CORDEX simulations for Africa have been used. In addition, we used ERA-Interim and CRU data to evaluate the CORDEX simulations. The results of this study can be summarized as follow:

- All the RCM members and their ensemble mean are able to reproduce the spatial distribution of the air temperature and wind speed over West Africa. Nevertheless, there is a bias between the RCM members and of the CRU and ERA-Interim.
- The ability of the CORDEX simulations to replicate the RSDS over West Africa is poor. In other words, the RCM members are not able to replicate the spatial distribution of RSDS over West Africa. The models overestimate the RSDS over West Africa and the bias goes up to 200 $W/m^2$.
- The variation of the air temperature of the RCM members and their ensemble mean over Ouagadougou is able to capture the mean of surface wind speed. While the CORDEX simulations overestimate the RSDS, most of them underestimate the air temperature.

- For both RCPs and global warming levels, all the RCMs project a warming over West Africa with a warming core over the Sahel region. Nonetheless, this warming in more accentuated in the 2 °C and under RCP 8.5.
- There is no agreement on the projection of surface wind speed, RSDS and PV potential over West Africa under RCP 4.5 and RCP 8.5 for 1.5 and 2 °C global warming level.
- On the daily basis, Ouagadougou may know an increase in air temperature for both RCPs and global warming levels.
- 50% of the daily data of surface wind, RSDS and PV potential agree that, no variation is observed in their change for RCP 4.5 and RCP 8.5 and both global warming levels. However, 75% and 25% agree in the variation.

The results of this study may help policy-makers in Burkina Faso. This study can be extended in many cities in Burkina Faso where we have a solar plant project. Moreover, the study in Ouagadougou is done on a daily basis; it can be enhanced by taking into account monthly, seasonal and yearly variation of the PV potential. This work can be enriched by adding more RCMs from CORDEX simulations and also by analyzing the multi-model multi-ensemble of the RCMs. Nonetheless, the RCMs used in this study revealed the ability of the CORDEX simulations to replicate the spatial distribution of air temperature and surface wind speed over West Africa.

# REFERENCES


Jeune Afrique. (2016). Burkina : les priorités d'Alpha Oumar Dissa, nouveau ministre des Mines et de l'Énergie. Retrieved October 10, 2017, from http://www.jeuneafrique.com/294066/economie/burkina-les-priorites-dalpha-omar-dissa-le-nouveau-ministre-des-mines-et-de-lenergie/

AMCEN. (2011). *Addressing Climate Change Challenges in Africa: A Pratical Guide towards Sustainable Development*.

Bharam, V. (2012). Advantages and challenges of silicon in the photovoltaic cells, (May).

Burnett, D., Barbour, E., & Harrison, G. P. (2014). The UK solar energy resource and the impact of climate change. *Renewable Energy*, *71*, 333–343. https://doi.org/10.1016/j.renene.2014.05.034

Cañete, C., Carretero, J., & Sidrach-de-cardona, M. (2014). Energy performance of different photovoltaic module technologies under outdoor conditions. *Energy*, *65*(April), 295–302. https://doi.org/10.1016/j.energy.2013.12.013

Crook, J. A., Jones, L. A., Forster, M., & Crook, R. (2011). Environmental Science Climate change impacts on future photovoltaic and concentrated solar power energy output. *Energy & Environmental Science*, 3101–3109. https://doi.org/10.1039/c1ee01495a

Davy, R., & Esau, I. (2014). Global climate models' bias in surface temperature trends and variability. *Environmental Research Letters*, *9*(11), 114024.

Déqué, Michel and Calmanti, Sandro and Christensen, Ole Bøssing and Aquila, Alessandro Dell and Maule, Cathrine Fox and Haensler, Andreas and Nikulin, Grigory and Teichmann, C. (2017). A multi-model climate response over tropical Africa at +2 °C. *Climate Services*, *7*, 87–95. https://doi.org/10.1016/J.CLISER.2016.06.002

Diallo, I., Sylla, M. B., Giorgi, F., Gaye, A. T., & Camara, M. (2012). Multimodel GCM-RCM ensemble-based projections of temperature and precipitation over West Africa for the early 21st century. *International Journal of Geophysics*, *2012*.

Diffenbaugh, N. S., & Giorgi, F. (2012). Climate change hotspots in the CMIP5 global climate model ensemble, 813–822. https://doi.org/10.1007/s10584-012-0570-x

Dimitri, S., Buri, Y., Lawin, E. A., & Coulibaly, O. (2016). Forecasted Changes in West Africa Photovoltaic Energy Output by 2045. *Climate*, 1–15. https://doi.org/10.3390/cli4040053

Dinc, F. (2011). The analysis on photovoltaic electricity generation status , potential and policies of the leading countries in solar energy, *15*, 713–720. https://doi.org/10.1016/j.rser.2010.09.026

Faso, F. contract N. 2015-A.-001-15DDU0C006-C.-S. F.-B. (2015). *Intended Nationally Determined Contribution (INDC) In Burkina Faso*.

Garg, H. P. (1974). Effect of dirt on transparent covers in flat-plate solar energy collectors. *Solar Energy*, *15*(4), 299–302. https://doi.org/10.1016/0038-092X(74)90019-X

Giorgi, F., Jones, C., & Asrar, G. R. (2009). Addressing climate information needs at the regional level : the CORDEX framework, *58*(July), 175–183.

Hamdy K. Elminir, ıtˇ ezslav Benda, J. T. r´ sek. (2001). EFFECTS OF SOLAR IRRADIATION CONDITIONS

AND OTHER FACTORS ON THE OUTDOOR PERFORMANCE OF PHOTOVOLTAIC MODULES. *Journal of ELECTRICAL ENGINEERING*, *52*(5), 125–133.

Harcourt, P. (2009). Effects of Temperature , Solar Flux and Relative Humidity on the Efficient Conversion of Solar Energy to Electricity, *35*(2), 173–180.

Harrison, G. P., & Wallace, A. R. (2005). Climate change impacts on renewable energy--is it all hot air? In *World Renewable Energy Congress (WREC2005), 22-27 May 2005, Aberdeen*. inproceedings.

Hu, A., Levis, S., Meehl, G. A., Han, W., Washington, W. M., Oleson, K. W., … Strand, W. G. (2016). Impact of solar panels on global climate, *6*(March). https://doi.org/10.1038/NCLIMATE2843

Jerez, S., Tobin, I., Vautard, R., Montávez, J. P., López-Romero, J. M., Thais, F., … others. (2015). The impact of climate change on photovoltaic power generation in Europe. *Nature Communications*, *6*, 10014.

Karl, T. R., Karl, T. R., & Trenberth, K. E. (2008). Modern Global Climate Change, *1719*(2003). https://doi.org/10.1126/science.1090228

Kerkhoff, C., Künsch, H. R., & Schär, C. (2014). Assessment of bias assumptions for climate models. *Journal of Climate*, *27*(17), 6799–6818. https://doi.org/10.1175/JCLI-D-13-00716.1

Mani, M., & Pillai, R. (2010). Impact of dust on solar photovoltaic ( PV ) performance : Research status , challenges and recommendations. *Renewable and Sustainable Energy Reviews*, *14*(9), 3124–3131. https://doi.org/10.1016/j.rser.2010.07.065

Meinshausen, M., Meinshausen, N., Hare, W., Raper, S. C. B., Frieler, K., Knutti, R., … Allen, M. R. (2009). Greenhouse-gas emission targets for limiting global warming to 2 6 C. *Nature*, *458*(7242), 1158–1162. https://doi.org/10.1038/nature08017

Ministere de l'Energie. (2016). [ Burkina Faso ]: Evaluation rapide et analyse d ’ écart.

Monerie, P., Roucou, P., & Fontaine, B. (2013). Mid-century effects of Climate Change on African monsoon dynamics using the A1B emission scenario, *896*(March 2012), 881–896. https://doi.org/10.1002/joc.3476

Ndiaye, A., Kébé, C. M. F., Ndiaye, P. A., Charki, A., Kobi, A., & Sambou, V. (2013). Impact of dust on the photovoltaic ( PV ) modules characteristics after an exposition year in Sahelian environment : The case of Senegal, *8*(21), 1166–1173. https://doi.org/10.5897/IJPS2013.3921

Prof Edenhofer Ottmar. (2011). *The IPCC Special Report on Renewable Energy Sources and Climate Change Mitigation*.

Riahi, K., Rao, S., Krey, V., Cho, C., Chirkov, V., & Fischer, G. (2011). RCP 8 . 5 — A scenario of comparatively high greenhouse gas emissions, 33–57. https://doi.org/10.1007/s10584-011-0149-y

Sagadevan, S. (2013). RECENT TRENDS ON NANOSTRUCTURES BASED SOLAR ENERGY APPLICATIONS : A REVIEW, *34*, 44–61.

Said, S., Massoud, A., Benammar, M., & Ahmed, S. (2012). A Matlab/Simulink-based photovoltaic array model employing SimPowerSystems toolbox. *Journal of Energy and Power Engineering*, *6*(12), 1965. article.

Sharma, S., Jain, K. K., & Sharma, A. (2015). Solar Cells : In Research and Applications — A Review, (December), 1145–1155.

Su, X., Takahashi, K., Fujimori, S., Hasegawa, T., Kato, E., Shiogama, H., … Emori, S. (2017). Earth ' s Future Emission pathways to achieve 2 . 0 ∘ C and 1 . 5 ∘ C climate targets Earth ' s Future. *Earth's Future*. https://doi.org/10.1002/eft2.211

Sui, Y., Lang, X., & Jiang, D. (2014). Time of emergence of climate signals over China under the RCP4 . 5 scenario. *Climatic Change*, 265–276. https://doi.org/10.1007/s10584-014-1151-y

Sulaiman, S. A., Hussain, H. H., Siti, N., Leh, H. N., & Razali, M. S. I. (2011). Effects of Dust on the Performance of PV Panels. *International Journal of Mechanical, Aerospace, Industrial, Mechatronic and Manufacturing Engineering*, *5*(10), 2028–2033.

Sylla, M. B., Elguindi, N., Giorgi, F., & Wisser, D. (2016). Projected robust shift of climate zones over West Africa in response to anthropogenic climate change for the late 21st century. *Climatic Change*, *134*(1), 241–253. https://doi.org/10.1007/s10584-015-1522-z

TamizhMani, G., Ji, L., Tang, Y., Petacci, L., & Osterwald, C. (2003). Photovoltaic module thermal/wind performance: long-term monitoring and model development for energy rating. In *NCPV and Solar Program Review Meeting Proceedings, 24-26 March 2003, Denver, Colorado (CD-ROM)*.

Tanoto, Y., & Handoyo, E. A. (2015). Renewable Energy Potential for Sustainable Long- Term Electricity Energy Planning : A Bottom-up Model Application, *5*(3).

Vilar. (2012). Renewable energy in West Africa. Retrieved December 15, 2017, from http://www.ecreee.org/sites/default/files/renewable_energy_in_west_africa_0.pdf

Villages, S. (2016). Energy Situation Report – West Africa. Retrieved September 28, 2017, from http://e4sv.org/wp-content/uploads/2016/10/West-Africa-Energy-Report-AW-Draft-3-200516-V3_MT.pdf

WETHE, J. (2009). *Energy Systems : Vulnerability-Adaptation-Resilience*.

Wild, M., Folini, D., Henschel, F., & Fischer, N. (2015). ScienceDirect Projections of long-term changes in solar radiation based on CMIP5 climate models and their influence on energy yields of photovoltaic systems, *116*, 12–24. https://doi.org/10.1016/j.solener.2015.03.039